



Cite this: *Polym. Chem.*, 2020, **11**, 5914

## A comprehensive review of the structures and properties of ionic polymeric materials

Jean-Emile Potaufeux,<sup>†[a,b](#)</sup> Jérémie Odent,<sup>†[a](#)</sup> Delphine Notta-Cuvier,<sup>b</sup> Franck Lauro<sup>\*[b](#)</sup> and Jean-Marie Raquez <sup>ID [\\*](#)[a](#)</sup>

Dynamic materials, which include ionic polymeric materials, contain specific bonds or interactions that can reversibly break and reform under certain stimuli or conditions. Among them, ionic polymeric materials leverage the dynamic and reversible nature of electrostatic interactions. Ionic motifs endow the materials with appealing stimuli-responsive properties such as shape-memory, self-healing or mechanical energy dissipation, thereby offering the possibilities to face current challenges such as recycling, fatigue resistance or material reinforcement. The present review first introduces the general concept of dynamic materials between the distinction of associative and dissociative dynamic networks in order to enlighten the unique properties of ionic polymeric materials. A particular emphasis is placed on the understanding of mechanistic principles controlling these reversible mechanisms. The latest developments in the field of ionic polymeric materials, including ionomer, polyelectrolyte and ionic hydrogel subclasses are further exhibited. After presenting the structure–property relationships and characteristics of recent ionic polymeric materials, the discussion extends to an overview of the applications of such systems.

Received 27th May 2020,

Accepted 18th August 2020

DOI: 10.1039/d0py00770f

[rsc.li/polymers](http://rsc.li/polymers)

<sup>a</sup>Laboratory of Polymeric and Composite Materials (LPCM), Center of Innovation and Research in Materials and Polymers (CIRMAP), University of Mons (UMONS), Place du Parc 20, 7000 Mons, Belgium.  
E-mail: [jean-marie.raquez@umons.ac.be](mailto:jean-marie.raquez@umons.ac.be)

<sup>b</sup>Laboratory of Industrial and Human Automatic Control and Mechanical Engineering (LAMIH), UMR CNRS 8201, University Polytechnique Hauts-De-France (UPHF), Le Mont Houy, 59313 Valenciennes, France. E-mail: [franck.lauro@uphf.fr](mailto:franck.lauro@uphf.fr)  
†These authors contributed equally to this work.



Jean-Emile Potaufeux

Jean-Emile Potaufeux obtained his Master's degree in Polymer Engineering at the University of Strasbourg, France in 2017, and his Engineering Degree in Polymer Chemistry at the European School of Polymer, and Materials Chemistry (ECPM). Since 2017, he has been a Ph.D. student in both the Laboratory of Polymer and Composite Materials (LPCM), University of Mons, Belgium and the Mechanical Department of

Laboratory of Industrial and Human Automatic Control and Mechanical Engineering (LAMIH), University Polytechnique des Hauts-de-France, France. His current research areas are the design of new ionic nanocomposites, and smart ionic polymer materials.



Jérémie Odent

Jérémie Odent received his Ph.D. from University of Mons (Belgium) in 2014 working on high-impact polylactide-based nanocomposites. He began working as a postdoc at Cornell University (United States) on designing novel ionic nanocomposites in 2015, and moved to his current position as a lecturer at UMons in 2017. Since then, he has developed new capabilities at the Laboratory of Polymeric Materials and Composites in the area of smart polymeric materials

and additive manufacturing technologies. Among recent investigations, he designed new 3D-printed polymeric inks capable of forming tough structural elements and providing novel electrical and optical functionalities for sensing and soft robotic applications.

# 1. Introduction to dynamic interactions: fundamentals of ionic polymeric materials

Over the past decade, dynamic materials, wherein specific bonds or interactions can reversibly break and reform under certain conditions, have gained widespread attention.<sup>1–3</sup> This concerns covalent (e.g. Diels–Alder cycloadducts,<sup>4</sup> disulfides,<sup>5</sup> boronic derivatives,<sup>6</sup> etc.) and non-covalent bonds (e.g. hydrogen bonding,<sup>7,8</sup> ionic interactions,<sup>9,10</sup>  $\pi$ – $\pi$  stacking,<sup>11</sup> metal-ligand coordination,<sup>12,13</sup> etc.). Introducing such reversible interactions into polymeric materials endows the system with multi-responsiveness including shape-memory,<sup>14,15</sup> self-healing,<sup>5,16</sup> mechanochromy,<sup>17</sup> or even electroactivity.<sup>16</sup> Referred to as stimuli-responsive, dynamic materials are truly capable of altering their chemical and/or physical properties upon exposure to external stimuli such as temperature, pH, water, light, stress or even electric fields,<sup>18,19</sup> though, a rapid bond exchange occurs either by an associative or dissociative pathway. In an associative pathway, bond breaking and reformation occur concomitantly (Fig. 1), whereas in a dissociative pathway (relative to ionic exchanges), the linkage dissociates first and then reforms after some time at a different location (Fig. 1). Note that following the type of interaction, a certain energy barrier needs to be reached in order to activate the breaking/reforming mechanisms (Fig. 2). For instance, a range of a few to 50  $\text{kJ mol}^{-1}$  is required in the case of weak interactions such as hydrogen bonding or  $\pi$ – $\pi$  stacking, whereas the activation energy of covalent bonds is on the order of a thousand  $\text{kJ mol}^{-1}$ .<sup>20</sup> Among these systems, Leibler *et al.* reported a radically new class of dynamic polymers based on associative mechanisms, called vitrimers.<sup>21</sup> They consist of covalent networks, which can change their topology by thermally activated bond-exchange reactions. Such a system can then flow (accord-

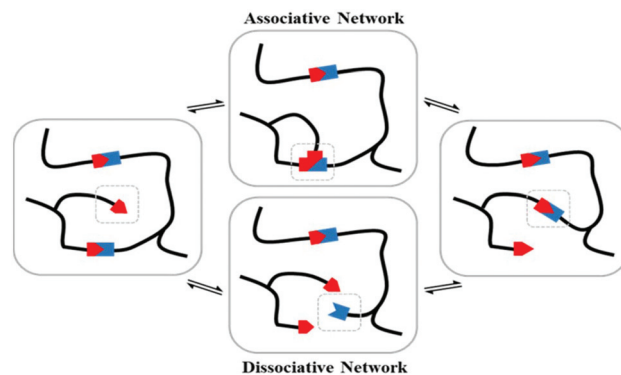


**Fig. 1** Representation of associative and dissociative network mechanisms. Adapted with permission from ref. 24. Copyright 2018, American Chemical Society. Adapted from ref. 22 with permission from the Royal Society of Chemistry, copyright 2015.

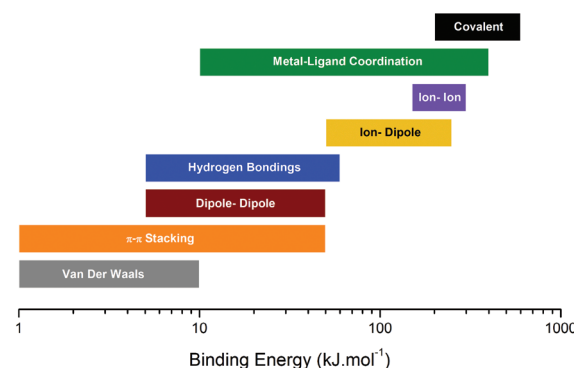


**Fig. 2** Summary of binding energies for different interactions. Adapted with permission from ref. 20. Copyright 2017, The Society of Rheology. Adapted from ref. 61 with permission from the Royal Society of Chemistry, copyright 2018.



**Delphine Notta-Cuvier**

*Delphine Notta-Cuvier received her Ph.D. in 2011 from the University of Valenciennes (France) for her work on the Virtual Fields Method for the characterization of viscoplastic behaviour. Since 2014, she has been an Assistant Professor in the Mechanical Department of LAMIH, in Valenciennes (France). Her research fields include in particular the multi-scale characterization and modelling of the mechanical behaviour of materials, especially polymers and reinforced polymers, from quasi-static to high-strain rate (crash) loadings. Thanks to a fruitful collaboration with her colleagues of the University of Mons, her research fields have been recently extended to the characterization of smart ionic polymeric materials.*

*behaviour of materials, especially polymers and reinforced polymers, from quasi-static to high-strain rate (crash) loadings. Thanks to a fruitful collaboration with her colleagues of the University of Mons, her research fields have been recently extended to the characterization of smart ionic polymeric materials.*

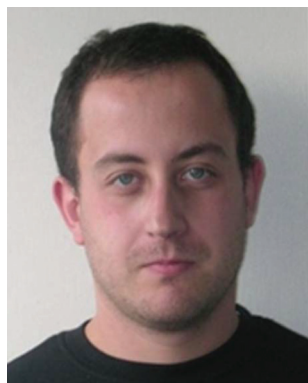


**Franck Lauro**

*Franck Lauro received his Ph.D. in 1996 from The University of Valenciennes (France) for his work on the modelling of damage behaviour of metals in crash. He was promoted to Professor in 2003 at the University of Valenciennes and he became the co-director of the Mechanical Department of the CNRS Laboratory LAMIH in Valenciennes in 2019. Since 2003, his research interests are mainly the characterization and*

*modelling of the behaviour, damage and failure of polymers and reinforced polymers under dynamic loading.*

ing to the Arrhenius law) above the topology freezing transition temperature ( $T_v$ ), whereas the bond-exchange reactions are nearly frozen at low temperature, so that vitrimers behave like classical thermosets.<sup>22</sup> Vitrimers are developed when transesterification,<sup>23,24</sup> transamination,<sup>25</sup> transalkylation,<sup>26</sup> and disulfide exchange<sup>17</sup> reactions are introduced and controlled. Most vitrimer-like systems use catalysts to activate or accelerate the breaking and restoration of reversible covalent bonds. The exchange rate is enhanced with the addition of a catalyst and a higher catalyst-to-crosslinker ratio, while the crosslink density governs the overall properties below the glass transition temperature ( $T_g$ ). These properties have been observed for vitrimers made of different matrices, *e.g.* poly(lactide) (PLA),<sup>27</sup> polycarbonate (PC),<sup>28</sup> polyurethane (PU)<sup>29</sup> or polyepoxy based on the diglycidyl ether of bisphenol F.<sup>30</sup> Such behavior is assigned to the duality of vitrimers, characterized by a “frozen” thermoset topology at low temperature and fast bond-exchanges above  $T_v$ . Ionic interactions incorporated into vitrimer structures have recently been used also to accelerate and improve these covalent bond exchanges.<sup>31,32</sup> Other methods such as introducing defects within the network (loop interactions)<sup>33</sup> or being away from the chemical equilibrium can be the main vectors to allow faster exchanges. For example, Liu *et al.* designed a vitrimer with improved dynamic properties (stress-relaxation and self-healing) by being far from the equimolar ratio between amine and epoxy groups.<sup>34</sup> Although the variety of vitrimers has become broader, only a limited number of associative chemical systems have been currently developed for designing vitrimer-like materials. Most of the existing vitrimers are used as self-healing systems, providing healing ability at high temperature while maintaining their intrinsic properties during the healing process. Up to now, the main challenges for future vitrimer development and emerging applications are their reprocessability by traditional means such as extrusion technology and their degradation resistance during material processing at high temperature.



Jean-Marie Raquez

Prof. Jean-Marie Raquez, a senior FRS-FNRS research associate, is the head of the Laboratory of Polymer and Composite Materials (LPCM) at the University of Mons in Belgium (see <http://smpc2017.bluehorizon.be/> for details) and scientific leader at the Applied Research Center Materia Nova in Belgium. His main research areas range from controlled and catalyzed polymerization reactions to production of high performance nanocomposites/nanohybrids via reactive processing, *e.g.* reactive extrusion, with a special emphasis on biobased plastics with key properties including shape-memory polymers and self-healing materials. He is an author of about 170 peer-reviewed publications, 11 patents, and 6 book chapters.

performance nanocomposites/nanohybrids via reactive processing, *e.g.* reactive extrusion, with a special emphasis on biobased plastics with key properties including shape-memory polymers and self-healing materials. He is an author of about 170 peer-reviewed publications, 11 patents, and 6 book chapters.

While the concept of reversible covalent bonds brings new properties to classical thermosetting polymer formulations in terms of processing options and recycling ability, the diversity of non-covalent chemistry together with a high degree of control over their binding mechanisms offer an almost endless number of possibilities to design advanced materials with tailor-made properties. In comparison with associative dynamics, dissociative systems can rapidly break and reform under mild conditions, in which it is unnecessary to use a catalyst to speed up these exchanges. However, the high reversibility of dissociative interactions usually goes with a lack of control over these exchange reactions and the resulting materials are not mechanically strong. It is commonly accepted to combine several of these types of interactions to take advantage of different reversible mechanisms (*i.e.* exchange rate and bond lifetime), conferring multi-responsive properties. Among all dissociative interactions, ionic systems differentiate from other polymeric materials as the resulting electrostatic interactions can be easily tuned and controlled by adequately choosing the nature, charge density and ionic strength of ions and counterions.<sup>35,36</sup> In the present paper, we aim at reviewing the latest developments in this field by focusing on ionic polymeric materials, including recent advances in the application of ionomers, polyelectrolytes and ionic hydrogels. The review also provides more in-depth discussions on the mechanistic pathways of dissociative interactions as described above and highlights ionic interaction dynamics. Finally, the review will focus on the recent outcomes concerning structure–property relationships and characteristics of the different categories of ionic polymeric systems and their applications.

## 2. Mechanistics of dissociative networks

In contrast to associative interactions, the dissociative pathway refers to an interchange mechanism in which the bonds break apart first and subsequently form new bonds at another position, after a certain time lag. The latter endows the materials with easy reprocessability at relatively low temperature, together with improved recyclability. Interestingly, the diversity of accessible dissociative interactions and their potential combinations offer a broader range of properties than most of the associative-like materials. Usual strategies used to investigate the dynamics of dissociative systems (and associative networks) are based on rheology, creep and stress-relaxation measurements.

Several studies based on simulation of the mechanical response of ionic materials permitted a more-in-depth mechanistic understanding of the dissociative interactions within polymeric materials.<sup>37,38</sup> Such investigations aimed at developing theoretical models to predict stress during loading–unloading cycles based on a fit with experimental data. While mechanistic theories are mainly built to model ionic interactions, most of them are adaptable to other types of dissociative networks. Note, though, that most of these investigations have been performed on dual network (DN) hydrogels. Recall that DN hydrogels are built of a permanent

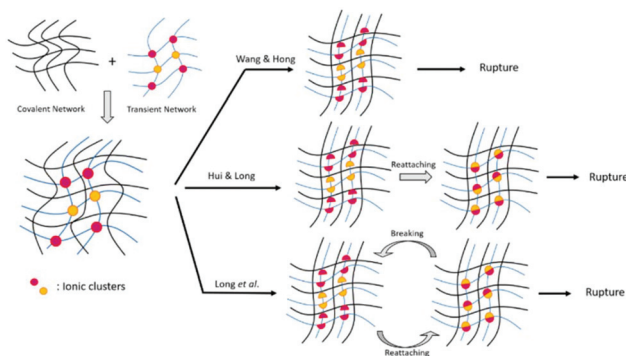


Fig. 3 Summary of first mechanistic models for DN hydrogels built on ionic interactions.<sup>38–40</sup>

covalently crosslinked network and another physically cross-linked network (commonly ionic network) (Fig. 3). Hyper-elasticity (*ca.* elastic response to very large strains, with a nonlinear stress–strain relationship), and a high level of energy dissipation are thereby achieved. However, classic viscoelastic models are hardly appropriate to describe DN hydrogel behavior. A model was first introduced by Wang *et al.* to describe DN hydrogel behavior and gradual damage.<sup>39</sup> The partial fracture of the transient network is herein believed to be the main cause of the high toughness of ionic DN hydrogels. However, for modelling purposes, authors considered the physically crosslinked network as being non-reversible after rupture (Fig. 3). Such a model was able to follow damage evolution and pseudo-elasticity of the material, showing two separate steps, namely (1) softening due to the fracture of the transient network and (2) extension of the stretching limit induced by the permanent network. Following this work, Hui, Long *et al.* introduced the idea that weak bonds could break and reattach in order to explain hysteresis and plasticity during loading–unloading cycles (Fig. 3).<sup>40</sup> By taking into account the reattachment of ionic crosslinks after breaking and stress-dissipation, this model was able to justify toughening and rate-dependent behaviors as well as self-healing ability. Such a model of DN hydrogels was the first one giving access to the dissipation energy due to transient network rupture and being extendable to multi-network gels. Later, Mayumi *et al.* succeeded in deconvoluting strain and strain-rate (*i.e.* time) effects over a wide range of elongation ratios ( $\lambda$ ) and strain rates during tensile testing.<sup>37</sup> A master curve of reduced stress function ( $f^* = \sigma/(\lambda - \lambda^2)$ , where  $\sigma$  is the nominal stress) was further obtained and it proved that  $f^*$  is only time-dependent before strain hardening. In this way, stress could be decomposed into a strain-dependent component, related to rubber elasticity, and another time-dependent component, related to the failure of transient crosslinks. Therefore, nominal stress function could be redefined with  $f^*(t)$  seen as a time-dependent elastic modulus during uniaxial stretching, though, this model suffered from some limitations assigned to the relaxation time of physical crosslinks. Authors thereby showed that DN hydrogels are brittle above a strain rate threshold (*ca.*  $0.3\text{ s}^{-1}$  in the present study) because of insufficient time to reversibly break

and restore the bonds. Besides, separating strain and time components out of stress function is not valid for a strain stiffening regime because of the finite extensibility of polymer chains. Long *et al.* further developed a new model for understanding the dynamics of DN hydrogels.<sup>38</sup> Their model first disproved equations as-developed by Mayumi *et al.* as the nominal stress of the material reaches 0 kPa for a value of  $\lambda > 1$  during loading–unloading tests, showing the existence of non-dissipated strain, while Mayumi's model predicted  $\sigma = 0$  for  $\lambda = 1$  (Fig. 4). This difference added to the discontinuity of the stress curve between loading and unloading proved that the reduced stress function  $f^*$  must be further dependent on the strain history. Adapting their model, Long *et al.* developed a deeper theory based on the same assumption: transient crosslinks can reattach after breaking and relaxation.<sup>38</sup> This time, the kinetics of chain attachment and detachment as well as the strain history component for stress function are taken into account. In comparison with Hui and Long's model, this new model considers that reattached chains could break again, though, the breaking kinetics becomes time dependent and insensitive to deformation. By considering that original and reattached chains had different kinetics (*i.e.* reattached chains break faster than original ones), the model now permits us to perfectly fit loading–unloading experimental data (Fig. 4) as well as tensile and stress-relaxation testing. Even if high strain fitting is still a limitation due to the strain hardening effect, Long's model is versatile and can be applied to any other combination of non-covalent and covalent bonding. The latter model has inspired others, being used as a framework for novel models which are ultimately adapted to specific tests or materials.<sup>41</sup> Among them, Drozdov *et al.* upgraded Long's model by modelling viscoelasticity, together with a viscoplastic behavior of DN gels.<sup>42</sup> As far as the viscoplastic response is concerned, two mechanisms were defined based on the slip-page of chains of the covalent network. The first one is non-dissipative and proportional to the strain rate, while the

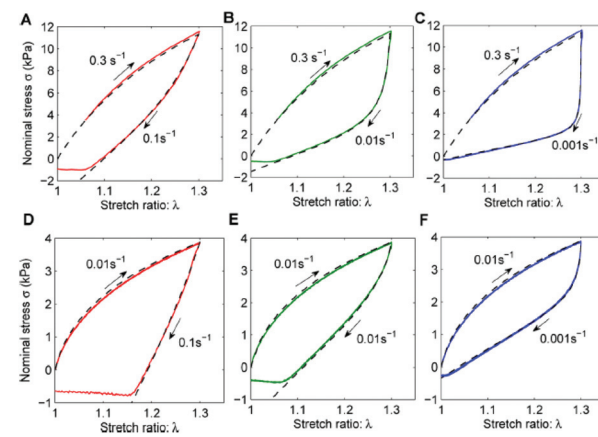


Fig. 4 Long *et al.* model fitting (dashed lines) with loading–unloading cycles (solid lines). Two loading rates are presented:  $0.3\text{ s}^{-1}$  (A–C) and  $0.01\text{ s}^{-1}$  (D–F). Unloading rate varies from  $0.1\text{ s}^{-1}$  (A and D) to  $0.001\text{ s}^{-1}$  (C and F). Reprinted with permission from ref. 38. Copyright 2014, American Chemical Society.

second one is a dissipative mechanism that depends on the chain interactions. Further models have been developed in order to study the stress softening phenomenon under quasi-static cyclic loading, also called the Mullins effect.<sup>43</sup> This effect may be due to a variety of micro-mechanisms, *e.g.* chain rupture or desorption. Mao *et al.* built a complex model simulating a viscoelastic response at a large deformation of polyacrylamide-based hydrogels that are ionically crosslinked with alginate.<sup>44</sup> The experiments revealed a Mullins effect under loading-unloading experiments, as well as a rate sensitivity during loading. Even if model prediction fits well experimental data on a broad range of deformation, fracture behavior cannot be modelled here. Another model was thereby developed by Külcü *et al.* to provide a deep understanding of the micro-mechanisms responsible for the stress softening and self-healing behavior of similar polyacrylamide/alginate hydrogels.<sup>45</sup> Herein, strain softening is defined as a consequence of energy dissipation due to transient crosslink rupture and polymer chain orientation. The same model characterized self-healing based on a combination of 2 factors: heating energy and re-bonding kinetics. As far as self-healing is concerned, Yu *et al.* presented a mechanistic model to provide a fundamental understanding of the interfacial mechanism of self-healable materials based on diffusion-reaction theory.<sup>46</sup> The following theory was able to predict the mechanical behavior and the healing efficiency over time of neat and healed materials based on modelling of chain-length distribution and force-dependent kinetics of dynamic bonds. Despite good agreement with data obtained for several non-covalent reversible networks (*ca.* ionic bonding, hydrogen bonding, and olefin metathesis), the present theory suffers from a few limitations. A more realistic distribution of the chain length (*ca.* polymer chains of different lengths) and the use of a finite element simulation should allow better fitting and analysis of more complex geometries than uniaxial bars. It is worth noting that previous models used elastic (or hyper- or viscoelastic) models, like neo-Hookean or Gent models, to describe chain mechanics, which prevents characterization of complex molecular mechanisms (*ca.* self-healing) by directly linking macroscopic mechanical properties and polymer chain physics. In contrast, a statistical approach of the polymer chain distribution has been used to precisely define dynamic exchanges within the material in Vernerey's theory, dedicated to the description of complex mechanical responses under inelastic or large chain deformation of reversible polymer networks.<sup>47,48</sup> This method considers every possible distribution (*e.g.* length, orientation, *etc.*) of polymer chains without any limitation related to elastic models. By using thermodynamic principles and a distribution tensor, the authors managed to correlate the macroscopic response of the material with the global physical conformation of polymer chains. Extrapolation of Vernerey's theory confirmed the efficiency of the present approach to bind the microscopic network configuration and motions to macroscopic properties. Still, only a few theories exist to describe the mechanistic response of dynamic polymeric networks.<sup>49</sup> While most of them used ionic

DN hydrogels as reference materials to build their models, others used conventional polymer networks with transient crosslinks similar to Vernerey's theory.<sup>50</sup> Among these scarce works, Grindly *et al.* combined experimental data and modelling on dynamic hydrogels made of a simple physical network to identify energy dissipation modes depending on the metal-ligand interactions between a 4-arm poly(ethylene glycol) and different metals.<sup>12</sup> Using the basic parallel association of Maxwell elements to fit the relaxation spectrum, the authors managed to speed up relaxation times by modifying Cu<sup>2+</sup>/Ni<sup>2+</sup> or Zn<sup>2+</sup>/Ni<sup>2+</sup> ratios to a higher quantity of nickel cations. Such models describing the mechanistic behavior of dynamic polymers allow a better understanding of dissipation energy mechanisms together with their rheological properties at the macroscopic scale.<sup>51,52</sup> It is worth mentioning that all efforts made to model the mechanical behavior of DN hydrogels or ionic polymers are indicative of highly appealing properties, going from full shape-memory behavior to high energy dissipation compared to conventional thermoplastics or gels. As such, the following section will focus on the key parameters that govern the dynamics of ionic polymeric materials, and therefore their stimuli-responsive properties.

### 3. Toward the mechanisms of ionic dissociation

As is commonly known, ionic interactions appear between cationic and anionic species and their corresponding counterions. Two types of ionic interactions can be observed: either intrinsic interactions, corresponding to a pair of cationic and anionic polymeric functions, or extrinsic interactions, corresponding to an association of polymeric ionic motifs with their oppositely charged counterions. While the ionic polymeric chains (either anionic or cationic) act as rigid rods in the absence of oppositely charged ions due to electrostatic repulsion, adding salt forms extrinsic ionic interactions and allows polymer chains to collapse due to a charge screening mechanism.<sup>53</sup> Further increasing the counterion valence or the counterion size results in stronger ionic interactions (*i.e.* decrease of relaxation time due to fast exchanges).<sup>54</sup> The opposite behavior is observed for polymers containing both positive and negative charges (*e.g.* polyampholytes and polyzwitterions) due to their intrinsic ionic interactions, commonly known as the anti-polyelectrolyte effect.<sup>55</sup> When both intrinsic and extrinsic ionic interactions occur within a material, four different diffusion processes could be identified: (1) free-ion diffusion, corresponding to extrinsic exchanges, (2) site diffusion, which refers to a switch between intrinsic and extrinsic interactions, (3) self-exchange, where an ionic function replaces another one of the same polymer chain in an intrinsic interaction, and (4) polymer diffusion, relative to macromolecular motions (Fig. 5).<sup>56</sup> Dynamic properties of ionic materials rely on these diffusion processes and differ depending on the values of the diffusion coefficient, which shows dependence on parameters such as temperature, ionic strength, polymer concentration,

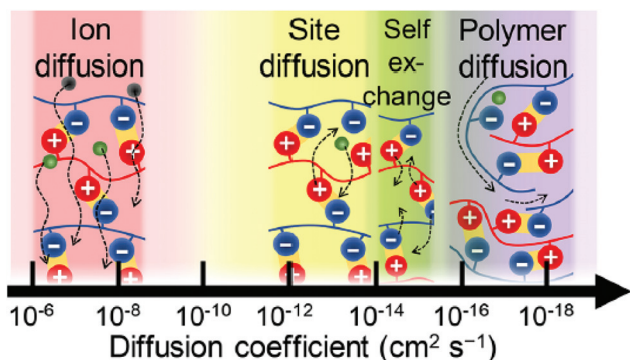


Fig. 5 Intrinsic and extrinsic diffusion processes within ionic polymer materials ranked according to their diffusion coefficients. Reprinted with permission from ref. 56. Copyright 2017, American Chemical Society.

and nature of ions and counterions. As an example, the addition of salt can lead to faster exchanges as a higher diffusion coefficient and thus a lower energy barrier are reached (Fig. 6).<sup>57</sup> It is established that when charged molecules interact together, the strength of ionic interactions is directly related to their respective  $pK_a$ .<sup>58</sup> Commonly used ionic motifs with respect to their  $pK_a$  are thereby listed in Fig. 7. The latter explains *e.g.* the weaker electrostatic interactions between an amine and a carboxylic acid against the same amine and a sulfonic acid. While weak ionic interactions have an extremely short lifetime due to their high reversibility, strong ionic interactions are expected to be more stable because of their high activation energy level. The energy activation herein describes how strongly two ionic motifs interact together. The required energy to break ionic interactions fully

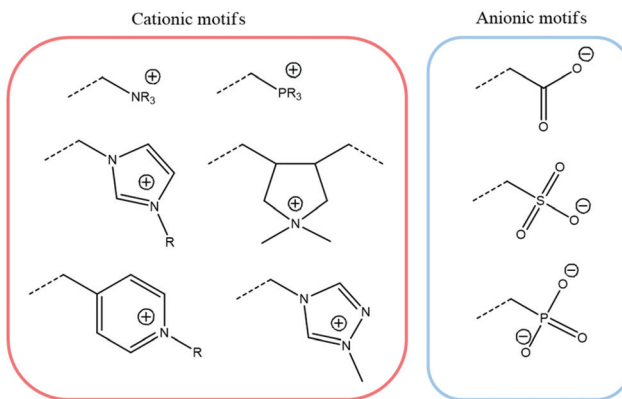


Fig. 7 Principal ionic motifs for the design of ionic polymeric materials.

controls the dynamics of ionic networks (*i.e.* exchange rate and bond lifetime). A broad range of energy activation can be achieved for ionic exchanges depending on many parameters such as ionic strength, counterions, or even the intermolecular distance between ionic motifs.<sup>59</sup> Thus, the lifetime of ionic bonds in aqueous solution can spread from milliseconds to tens of years.<sup>60</sup> This control of the strength of ionic interactions and the associated energy activation represents one of the key parameters for the development of a broad range of ionic polymeric materials. Besides, it offers a good compromise between the weakness of hydrogen bonding and strong covalent bonds. Based on their energy activation, electrostatic interactions are thereby associated with specific applications where fast recombination or stable interactions are needed. In other words, a combination of ionic interactions of various strengths is often used to design tough materials since reversible interactions will break at different stress levels. Note that the strength of ionic interactions might be measured by calculating relaxation times or energy activation.<sup>61</sup>

The distribution of ionic functions along the polymer chains is another key parameter to tailor the dynamic exchanges. Lytle *et al.* and Rumyantsev *et al.* herein highlighted that a perfect random distribution of cations along a polyelectrolyte sequence reduces the strength of coacervates, while multi-block sequences improve the association of electrostatic interactions and create denser, more salt-resistant coacervates.<sup>62,63</sup> In opposition to highly ionically functionalized polymers (*i.e.* polyelectrolytes), polymers with a lower amount of ionic functions (*i.e.* ionomers) show more ability to collapse due to less electrostatic repulsion forces.<sup>64</sup> Since less repulsive interactions are present within an ionomer, multiple ionic functions can interact with counterions at the same location, leading to the formation of ionic clusters. Note that charge delocalization stabilizes ionic clusters, thus locally strengthening electrostatic forces within these nanodomains.<sup>65</sup> Like polyelectrolytes, the architecture of ionomers strongly affects the morphology and therefore ionic interaction strength.<sup>66</sup> Ionic cluster structures (discrete or percolated) and shapes (globular, spherical, or disk) can be tuned depending

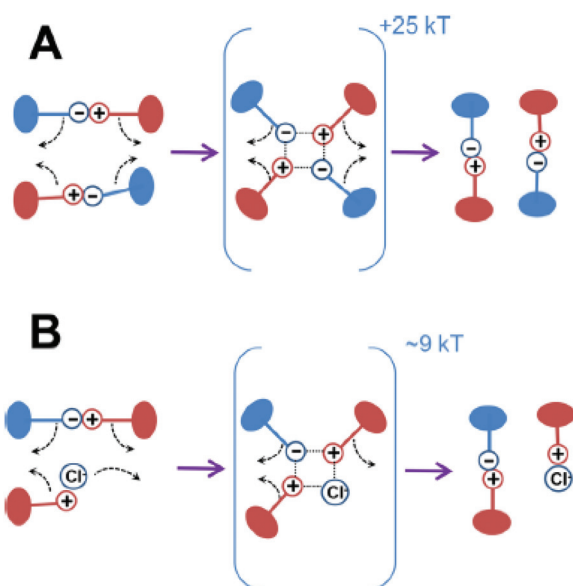


Fig. 6 Rearrangement of ionic interactions (A) in the absence of salt (intrinsic exchange), and (B) in the presence of salt counterions (extrinsic exchanges). Reprinted with permission from ref. 57. Copyright 2019, American Chemical Society.

on parameters such as the polymer architecture (linear, grafted or star-shaped polymers), distribution of ionic moieties (random, periodic, or telechelic) and ionic functions.<sup>66–68</sup> For instance, it has been theoretically and experimentally proven that the largest and strongest clusters are obtained for the telechelic architecture, while ionic clusters are smaller for ionomers with periodic distribution of ionic moieties compared to ionomers with random distribution.<sup>69</sup> It is therein obvious that the structures and compositions of ionic systems will have a strong impact on the underlying dynamic mechanisms, thus controlling the overall performance of ionic polymeric materials. While ionomers are characterized by their ionic aggregates (clusters) and polyelectrolytes by ion-pairing, few studies focused on the transition between ionomer and polyelectrolyte-like behaviors.<sup>70</sup> By adapting the amount of ionic moieties on a copolymer, Enokida *et al.* proved that a gradual transition occurred with the coexistence of both ion clusters and a continuous ionic phase.<sup>71</sup> They also observed that significantly increasing the size of counterions allowed ion cluster dissociation due to screened ionic interactions.<sup>72</sup> Other studies reported that ion aggregation could be enhanced by crosslinking or reducing backbone polarity, whereas plasticization led to ion dissociation.<sup>73,74</sup> With the large variety of ionic motifs and their controlled distribution along polymer chains, a broad range of ionic interaction energies can be achieved. Note that due to the interaction strength and their rapidity to rebond, some materials containing strong ionic interactions can show a behavior close to Arrhenius law under a stress-relaxation experiment (*i.e.* vitrimer-like behavior). However, to the best of our knowledge, up to now, no ionic polymeric systems have shown a purely associative-like (vitrimer-like) behavior. Indeed, associative systems are today only represented by covalent adaptive networks (CANs) in which the bonds break and reform simultaneously (leading to a constant cross-link density).<sup>49</sup> Nevertheless, the development of ionic polymeric materials built on strong ionic interactions might be a possible pathway to design new vitrimer-like materials or to take advantage of associative/dissociative double interaction systems.

#### 4. Classification of ionic polymeric materials

Ionic polymeric materials can be subdivided in three classes namely ionomers, polyelectrolytes and ionic hydrogels. Ionomers and polyelectrolytes are defined as charged polymers in which repeated ionic units are present respectively at low (from 1 to 15 mol%) and high concentrations (higher than 10 to 15 mol%). On the other hand, ionic hydrogels present physically (and chemically) crosslinked networks (made of ionomers or polyelectrolytes) that are able to hold a large amount of water by swelling. The following section will present these three classes of ionic polymeric materials and the role of reversible bonds will be revealed through specific physico-mechanical properties.

#### 4.1. Ionomers

Ionomers are defined as polymers where a fraction of repeated units contains an ionic functionality, usually in the range of 1 to 15 mol%. Eisenberg *et al.* proposed a more precise definition based on the overall properties of the material, defining ionomers as “polymers in which the bulk properties are governed by ionic interactions in discrete regions of the material”.<sup>75</sup> Herein, “discrete regions” referred to small aggregates formed by the association of numerous, tightly packed ionic groups, also called ionic clusters (Fig. 8). The effect of ionic bonding on the polymer structure was first evidenced by Rees, Vaughan *et al.* using commercial poly(ethylene-*co*-methacrylic acid)-based thermoplastic as-developed by Dupont™ under the name Surlyn®.<sup>76</sup> Surlyn® has been widely studied and has shown interesting mechanical and thermal-responsive properties. Driven by not only the crystallization process and thermal transitions, but also by the presence of ionic clusters within the materials, Surlyn® exhibits multiple shape-memory effects, and reversibly responds to temperature, *i.e.* expanding under cooling and shrinking under heating leading to the so-called “two-way reversible actuation”.<sup>15,77</sup> Besides, the self-healing ability of neat Surlyn® during ballistic penetration was investigated by Varley *et al.*<sup>78</sup> Herein, Surlyn® presents better self-healing and more elastomeric properties above its melting temperature ( $T_m$ ) due to the high mobility of ions within these ionic clusters.<sup>79</sup> Besides, better healing properties are obtained above the  $T_m$  by neutralizing the ionomer to a large extent with sodium cations (formation of ionic interactions and ionic clusters).<sup>80</sup> While common thermoplastics flow above their  $T_m$ , it is worth mentioning that ionomers preserve good mechanical stability due to the presence of ionic clusters. Post *et al.* thereby designed healable Surlyn®/magnetite nanoparticle blends.<sup>81</sup> Herein, the resulting nanocomposite heals when a magnetic field is applied on the material, inducing a local temperature change at the vicinity of damaged areas. Note also that increasing the local mobility of clustered ions (*e.g.* under heating or *via* plasticization) leads to better self-healing properties because of a faster reforming mechanism of ionic clusters.<sup>82</sup> It is worth mentioning that the overall properties of ionomers are driven by the size and size distribution of clusters, which are influenced by ionic density and the nature of counterions. Free-ions and ionic clusters are constantly in equilibrium. By adding or changing counterions ( $\text{Na}^+$ ,  $\text{Zn}^{2+}$ , *etc*), macroscopic modifications of ionomer properties are observed due to a displacement of free-ion/ionic

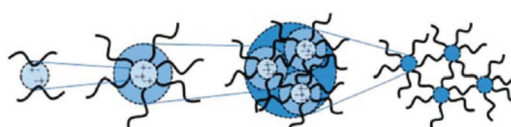


Fig. 8 Schematic representation of the hierarchical formation of the ionomer morphology. From left to right: ion pairs, multiplets, ionic clusters, and network. Reproduced from ref. 64 with permission from the Royal Society of Chemistry, copyright 2014.

cluster equilibrium.<sup>83</sup> For instance, neutralizing Surlyn® using sodium or potassium cations affects not only its crystallization and rheological properties but also its mechanical characteristics. As such, Qiao, Weiss *et al.* focused on the rheological behavior of sulfonate polystyrene, showing that the addition of metallic cations shifts the equilibrium in favor of clustered ion-pairs, which in turn increases the rigidity and melt viscosity.<sup>84</sup> Besides, Bose *et al.* correlated healing performances of poly(butyl acrylate) ionomers with the amount and type of metallic cations ( $\text{Na}^+$ ,  $\text{Co}^{2+}$ , and  $\text{Zn}^{2+}$ ) and observed faster reversible interactions of higher valence metal ions or increased ionic content.<sup>64,85</sup> In particular, they confirmed that the kinetics of cluster formation, as-controlled by the ionic content, was the limiting parameter to the healing kinetics compared to network relaxation. Note that, while clusters are commonly located in the amorphous phase, high concentration of clusters locally increases the stiffness and forms vitreous ion-rich regions (Fig. 9).<sup>86</sup> Due to the presence of ionic clusters avoiding chain rearrangement, ionomers usually have low crystallinity (<15%) and a low crystallization rate.<sup>83,87</sup>

Apart from Surlyn®, other commercially available ionomers have been developed such as Nafion®, a poly(tetrafluoroethylene) (PTFE)-based ionomer bearing sulfonate-ended pendant chains mainly used as a proton conductor for proton exchange membranes. Interestingly, Nafion® possesses multiple shape memory properties within a large range of temperatures.<sup>88</sup> Kohlmeyer *et al.* reported independently activated shape memory effects upon different stimuli (*i.e.* thermal and infrared and chemical stimuli) for Nafion®/carbon nanotube nanocomposites.<sup>89</sup> Besides, acrylic acid, methacrylic acid, and phosphonium groups likely represent the most common partners to design negatively charged ionomers. As such, Middleton *et al.* investigated the effect of lithium neutralization of poly(ethylene-*co*-acrylic acid) under stretching.<sup>90</sup> Herein, high ionic content, *i.e.* favoring interactions within ionic clusters, led to improved Young's modulus and yield stress. A similar effect was highlighted for phosphonate-functionalized poly(ethylene terephthalate) ionomers.<sup>91</sup> As far as cationic ionomers are concerned, imidazolium and quaternary ammonium-functionalized polymers are among the most representative ionic functions.<sup>92–94</sup> Interestingly, Odent *et al.* designed multi-

responsive nanocomposites based on imidazolium-functionalized PUs and well-defined sulfonate surface-modified silica nanoparticles.<sup>14,95</sup> Unlike previous ionomers, unique and unconventional strain-rate dependent behavior (*i.e.* simultaneous increase of Young's modulus, yield strength and strain at break with increasing strain rates) is observed. This new design also exhibited remarkable shape memory and self-healing characteristics.

#### 4.2. Polyelectrolytes

In contrast to ionomers, polyelectrolytes are charged polymers whose repeated ionic units are present at high concentration, usually higher than 10 to 15 mol%. Again, Eisenberg *et al.* further defined polyelectrolytes as “polymers in which solution properties (*i.e.* viscosity) in solvents of high dielectric constants are governed by electrostatic interactions over distance larger than typical molecular dimension”.<sup>75</sup> Note that polyelectrolytes are commonly classified as weak or strong depending on their ability to fully dissociate in solution. That is, mixing oppositely charged polyelectrolytes in aqueous solution forms polyelectrolyte complexes (PECs). Several types of complex formations can be observed such as macroscopic PECs, soluble complexes or micelles. As previously exposed, three major diffusion processes take place within PECs: (1) free-ion diffusion, (2) polymer reptation, and (3) local rearrangement of ionic repeated units, also called ionic site diffusion. The latter is responsible for PEC dynamics and is strongly influenced by temperature and ionic strength.<sup>56</sup> Remember that PEC properties are ruled out by intrinsic (between oppositely charged polyelectrolytes) and extrinsic (counterion/polyelectrolyte electrostatic interactions) exchanges. By investigating the linear viscoelastic response for a series of PECs made from different pairs of poly[3-(methacryloylamino)propyltrimethylammonium chloride] and poly(sodium methacrylate), Yang *et al.* demonstrated a faster ion-pair exchange rate between polyelectrolytes in the presence of salt.<sup>57</sup> It is well-known that charge density and ionic strength (*i.e.* salt concentration) influence the relaxation process (*i.e.* reversible formation/rupture) of PECs, which is a 2 step-process decomposed into (1) formation of an initial complex, and (2) rearrangement toward an equilibrium state.<sup>96</sup> The first step is driven by diffusion of ions with the release of counterions, while the second step is driven by an increase in configurational entropy. This second step is much slower since polyelectrolytes rearrange through exchange reactions toward an equilibrium state.<sup>97</sup> Usually, a fast relaxation process leads to liquid-like complexes, so-called complex coacervates. Note that weak polyelectrolytes tend to form these types of complexes, while strong polyelectrolytes (with slower relaxation due to stronger ionic interactions) tend to become solid PECs. Concerning weak polyelectrolytes, it is established that the dissociation (and association) process is influenced by the oppositely charged polyelectrolyte. Indeed, Rathee *et al.* highlighted that the local charge of a weak polyelectrolyte increased when in contact with the other oppositely charged polyelectrolyte, explaining the stabilization of complex coacervates due to local strong ionic interactions.<sup>98</sup> Nevertheless,

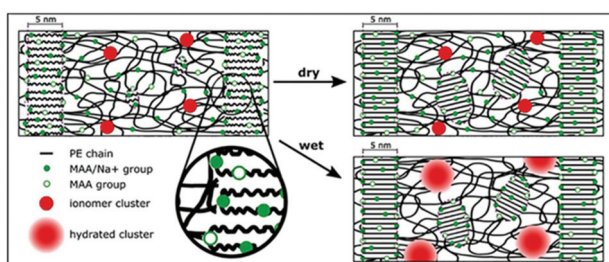


Fig. 9 Schematic morphological solid-state evolution of sodium neutralized poly(ethylene-*ran*-methacrylic acid) (E/MAA-Na<sup>+</sup>) ionomers under thermal annealing. Reprinted with permission from ref. 86. Copyright 1995, American Chemical Society.

mechanisms related to the formation of PECs made of weak polyelectrolytes are still not clearly elucidated.<sup>99</sup> In addition to salt-dependence, the polymer architecture affects the relaxation process and the final form of the PECs. For instance, multi-block sequences instead of random distribution of cations along a polyelectrolyte sequence strengthen electrostatic interactions and create more salt-resistant coacervates.<sup>62,63</sup> Besides, polyelectrolytes are highly ionic (or ionizable) polymers, so variation of acidity of the solution easily affects the interactions within PECs and leads to important modifications of the overall properties. Interestingly, chitosan/alginate self-assemblies can form either a fiber structure or colloidal nanoparticles in acidic or low basic solutions, respectively.<sup>100</sup> pH and thermo-responsiveness are also revealed for poly(*N*-isopropylacrylamide)/alginate-chitosan core-shell particles, also characterized by their excellent interface strength due to alginate–chitosan ionic interactions.<sup>101</sup> Interestingly, the higher the number of ionic groups along polyelectrolyte chains, the better the chain mobility and the faster the ionic exchanges. Song *et al.* thereby took advantage of electrostatic interactions between polyethyleneimine and polyacrylic acid to design a self-healable multilayered coating as-prepared by layer-by-layer deposition.<sup>102</sup> It is worth mentioning that the strong electrostatic interactions in the system permitted the reduction of the free-volume within the coating, leading to strong oxygen barrier properties.

Poly(ionic liquid)s (PILs) are a subclass of polyelectrolytes where the repetitive units are made of ionic liquids. High thermal and electrochemical stability, negligible vapor pressure, and high ionic conductivity are among the interesting properties of PILs. Based on the broad variety of available ionic liquids, a large range of chemical structures and architectures are accessible for designing PILs. Among these investigations, Erwin *et al.* compared viscoelastic and dielectric properties of linear and star-shaped imidazolium-based PILs, showing similar ionic conductivity but morphologies and rheological properties that can be tuned since linear PILs show lower melt viscosity and improved dynamics of ionic interactions.<sup>103</sup> Zhang *et al.* designed PIL-based nanoparticles from 1-vinyl-1,2,4-triazolium-type ionic liquids with a controllable shape and highly ordered internal morphologies.<sup>104</sup> Herein, the shape of the nanoparticles turned from “gasp-like” to “onion-like” upon the increase of the alkyl chain length on the triazolium moieties (*i.e.* by increasing the hydrophobicity). A porous membrane made of poly(imidazolium) ionically interacting with poly(acrylic acid) was designed by Wu *et al.*, and it showed recyclability using high ionic strength solutions.<sup>105</sup> Others developed thermo- and pH-responsive membranes based on PILs made of acrylic acid, *N*-isopropylacrylamide, acrylonitrile and butyl-imidazolium repetitive units (Fig. 10).<sup>106</sup> The resulting membrane is either transparent under heating or alkaline conditions, or twisted at a high pH value, depending on the predominance of hydrogen bonding or electrostatic interactions. Indeed, hydrogen bonding is dominant at room temperature while increasing the temperature or pH value intensifies ionic interactions within the PIL.

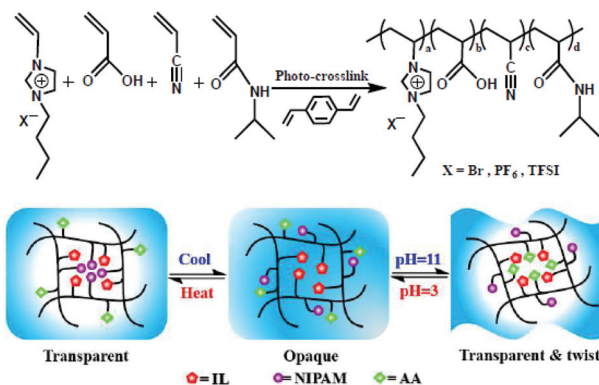


Fig. 10 Reaction scheme for the preparation of PIL-based membranes via *in situ* photo-crosslinking and their mechanism of thermo- and pH-responsive behaviors. Reproduced from ref. 106 with permission from the Royal Society of Chemistry, copyright 2016.

Polyampholytes (or amphoteric polyelectrolytes) are another subclass of polyelectrolytes, *i.e.* polymers with both anionic and cationic charges. In opposition to polyanions and polycations, polyampholytes are able to interact with themselves through intra-ionic interactions.<sup>36,107</sup> For instance, Peng *et al.* designed high-molecular-weight polyampholytes with high self-healing characteristics using butyl acrylate, acrylic acid and dimethylaminoethyl methacrylate as monomers.<sup>108</sup> Herein, a trade-off among toughness, stiffness and self-healing efficiency was reached thanks to the progressive rupture of ionic clusters and thus a high level of energy dissipation. Also, in opposition to purely cationic or anionic polyelectrolytes, polyampholytes show an “anti-polyelectrolyte effect”, which has been described as an increase of the viscosity of a polyelectrolyte solution by the addition of a low-molecular weight salt (Fig. 11).<sup>109</sup> Indeed, the rupture of intra-chain ionic interactions by the addition of salt results in an expansion of the polymer chains by disintegrating the ionic network.<sup>110</sup> Among polyampholytes, polyzwitterions (PZw) are characterized by an overall electrical charge of zero as they contain the same

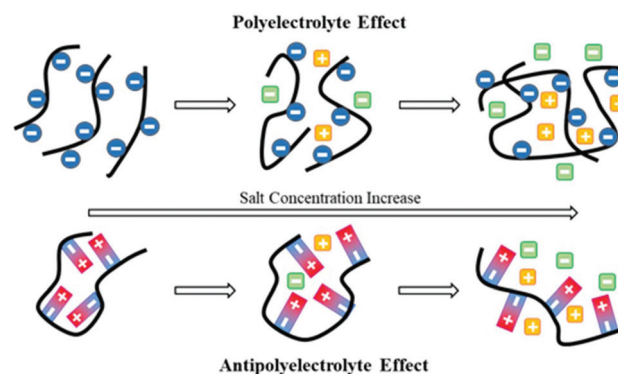
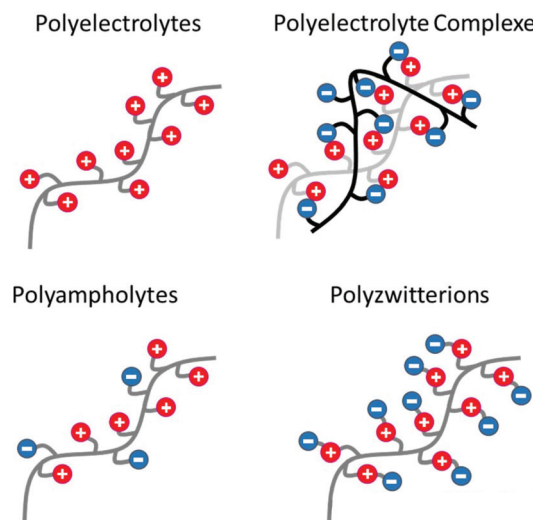


Fig. 11 Schematic representation of polyelectrolyte and antipolyelectrolyte effects. Cationic and anionic moieties are represented in red and blue, respectively, while salt ions are depicted as green and yellow squares.



**Fig. 12** Schematic representation of polyelectrolytes, polyelectrolyte complexes (association of oppositely charged polyelectrolytes), polyampholytes (polyelectrolytes bearing both cationic and anionic charges) and polyzwitterions (polyampholytes with the same amount of cationic and anionic functions on a repetitive unit).

number of cationic and anionic functions on a repetitive unit (Fig. 12). Gao *et al.* thereby compared the swelling properties of polyampholytes and polyzwitterions with different charge stoichiometric ratios but identical ionic moieties.<sup>111</sup> Higher swelling ratios are observed for balanced polyampholytes due to weaker inter-chain interactions compared to PZw. Indeed, PZw possesses stronger inter-chain ionic interactions based on the proximity of oppositely charged functions on PZw repetitive units. Moreover, Sun *et al.* designed ionogels made of polyzwitterion-based hydrogels bearing imidazolium and sulfonate moieties and swollen with an imidazolium-based ionic liquid.<sup>112</sup> Combining PZw and ILs within a single material allows maximization of electrostatic interactions (PZw–PZw and PZw–IL ionic interactions). Thereby, ion-based physical crosslinks endow the material with similar mechanical properties to covalently crosslinked gels. As the ionic liquids embedded within the ionogels act as a plasticizer, the final material is softer, though, able to self-heal and recover up to 80% of its original strength.

#### 4.3. Ionic hydrogels

Ionic hydrogels are physically crosslinked hydrogels bearing ionic motifs (made of ionomers or polyelectrolytes) that are able to hold a large amount of water by swelling. In opposition to covalently crosslinked hydrogels, ionic hydrogels show self-healing properties and high toughness. Taking advantage of reversible sacrificial bonds, ionic hydrogels can also overcome limitations related to softness and brittleness. For instance, Yuan *et al.* designed hydrogels that consist of a mixture of two polycations, *i.e.* (poly(diallyldimethylammonium chloride) (PDDA) and poly(ethyleneimine) (PEI)), and two polyanions, *i.e.* (poly(sodium 4-styrenesulfonate) (PSS) and poly(acrylic acid) (PAA)) (Fig. 13).<sup>113</sup> Combining several ionic polymers

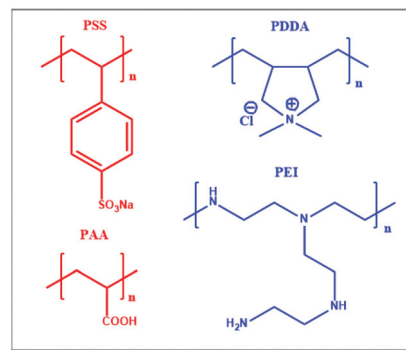


**Fig. 13** Ionic polymers used by Yuan *et al.* to design tough hydrogels. Adapted with permission from ref. 113. Copyright 2019, American Chemical Society.

with different acid dissociation constants ( $pK_a$ ) introduces electrostatic interactions of various strengths. The overall performance of the resulting hydrogels is driven by the (1) weak electrostatic interactions of all components, (2) strong ionic interactions between PDDA and PSS, resulting in nanodomain formation, and (3) hydrogen bonding between PEI and PAA. Combining such interactions within a single hydrogel endows the material with excellent self-healing and mechanical properties as well as recyclability after immersion in water. Many studies have reported the coupling of dissociative interactions (*e.g.* ionic bonding, hydrogen bonding, and metal-ligand coordination) or even associative and dissociative interactions.<sup>114–117</sup> Recently, Su *et al.* combined hydrogen bonding and ionic interactions within a poly(2-acrylamido-2-methyl-1-propanesulfonic acid)-based superabsorbent material.<sup>118</sup> While hydrogen bonding conferred high swellability and ductility, electrostatic interactions improved toughness and stiffness and endowed the material with self-healing ability. Note that another possibility to tune the ionic interaction strength is to vary the pH of the aqueous solution in which the hydrogel is swollen. It is worth mentioning that the overall properties of ionic hydrogels are strongly dependent on their swelling ability and on the pH of their environment. For instance, Afzal *et al.* studied the impact of pH on the rheological properties of chitosan/alginate hydrogels.<sup>119</sup> At pH values comprised between the  $pK_a$ s of polymers ( $4 < \text{pH} < 6$ ), full ionization of amine and carboxylic acid occurs and leads to highest viscosities and moduli, while  $\text{pH} > 6$  leads to increased brittleness. Moreover, it is possible to tune the softness and brittleness of these ionic hydrogels by changing alginate and chitosan concentrations. In parallel to hydrogels made of blends of oppositely charged polyelectrolytes, other ionic hydrogels are composed of polyampholytes. Such polyampholytes made of randomly distributed ionic moieties (as characterized by a wide range of ionic bond energies) surely represents a simple approach to design hydrogels with tunable mechanical properties.<sup>120</sup> Strong ionic interactions act as permanent crosslinks and maintain the macroscopic structure of the hydrogel, whereas weak interactions are reversible and

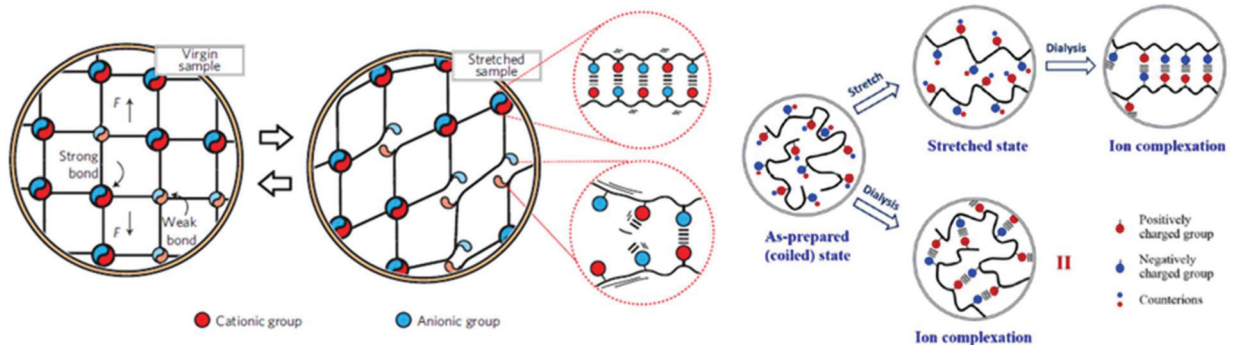


**Fig. 14** Scheme of weak and strong ionic interactions (left). Adapted with permission from ref. 120. Copyright 2013, Springer Nature. Representation of the pre-stretching effect on ion complexation (right). Reproduced from ref. 121 with permission from the Royal Society of Chemistry, copyright 2016.

confer toughness as well as fatigue resistance and self-healing ability (Fig. 14). Cui *et al.* herein proposed a method to improve the mechanical properties of ionic hydrogels by imposing pre-stretch and dialysis steps before tensile testing.<sup>121</sup> Thereby, polymer chains get oriented and aligned, resulting in stronger ionic interactions. This reinforcing effect is thought to arise from the higher strength of ionic interactions due to the greater proximity of ionic groups and polymer chain alignment. Note that this increase of stiffness also slightly reduces the dynamic behavior of the hydrogel since strong ionic interactions need more energy to break and reform. Besides, Fan *et al.* designed another polyampholyte-type hydrogel that combined multiple ionic, hydrophobic and metal-ligand coordination interactions to endow the resulting material with dual-responsive shape-memory properties.<sup>122</sup> Addition of metallic cations represents an easy way to tune hydrogel stiffness by favoring the coordination of acrylic acid on the metal, and thus lowering the amount of ionic interactions between acrylic acid and 2-(*N,N*-dimethylamino)ethyl methacrylate groups. Ionic hydrogels are further emerging through *in situ* polymerization of an electrolyte in a solution already containing an oppositely charged polyelectrolyte. For instance, ionic hydrogels designed by Wang *et al.* are based on *in situ* polymerized *p*-styrenesulfonate within poly[3-(methacryloylamino)propyl-trimethylammonium chloride] in saline (*i.e.* NaCl) solution.<sup>123</sup> The high mobility of sodium *p*-styrenesulfonate monomers in solution allows stronger ionic interactions after polymerization due to an improved proximity of oppositely charged polyelectrolytes. Yuan *et al.* used the same synthesis method to prepare PAA/cationic chitosan blends with high conductivity and self-healing characteristics.<sup>124</sup> Semi-interpenetrating networks (semi-IPN) can be further designed through the same procedure to obtain even stiffer hydrogels. Banerjee *et al.* thereby designed semi-IPN with self-healing and shape memory behaviors as well as electrical actuation depending on the hydrogen-to-ionic bonding ratio within the materials.<sup>125</sup> Such emerging properties of ionic polymeric materials dominated by non-covalent ionic interactions will be discussed in the following section.

## 5. Key properties of ionic polymeric materials

Key properties of ionic polymeric materials correspond to stimuli-responsive properties driven or affected by the presence of ionic interactions, such as shape-memory, self-healing, energy dissipation or ionic conductivity.

### 5.1. Shape-memory

Shape-Memory Polymers (SMPs) are an emerging class of polymers with applications spanning from medical devices and implants, self-deployable structures, fabrics, electronics, sensors to selective membranes.<sup>126,127</sup> SMPs can actively recover from a metastable state (*i.e.* temporary shape) to their original shape (*i.e.* permanent shape) when subjected to an external stimulus such as temperature,<sup>128</sup> humidity,<sup>129</sup> microwave,<sup>130</sup> electric or magnetic fields.<sup>131</sup> Herein, a shape-memory cycle includes three steps, namely (1) programming, *i.e.* applying a mechanical force to deform the material from its original shape to its temporary shape; (2) fixation, *i.e.* locking the temporary shape under a “frozen stage” after removing an applied stress, and possibly acting on the environment if necessary (*e.g.* cooling the material down); (3) recovery, *i.e.* partial or full restoration of the original shape upon application of an external stimulus. For each cycle, the strain fixity rate ( $R_f$ ) quantifies the ability to fix a mechanical deformation resulting in a temporary shape while the strain recovery rate ( $R_r$ ) quantifies the ability to restore the mechanical deformation of the permanent shape. Among possible stimuli, thermal treatment probably represents the easiest way to trigger shape-memory properties. Building on ionic motifs, ionic polymeric materials have the ability to endow the materials with thermally induced shape-memory characteristics.<sup>132</sup> Indeed, the reversible behavior of ionic interactions permits the breaking of the physical network upon heating (*i.e.* during programming and recovery steps) and its re-formation at lower temperature (*i.e.* fixation step). For instance, Wang *et al.* combined covalent and non-covalent crosslinks to

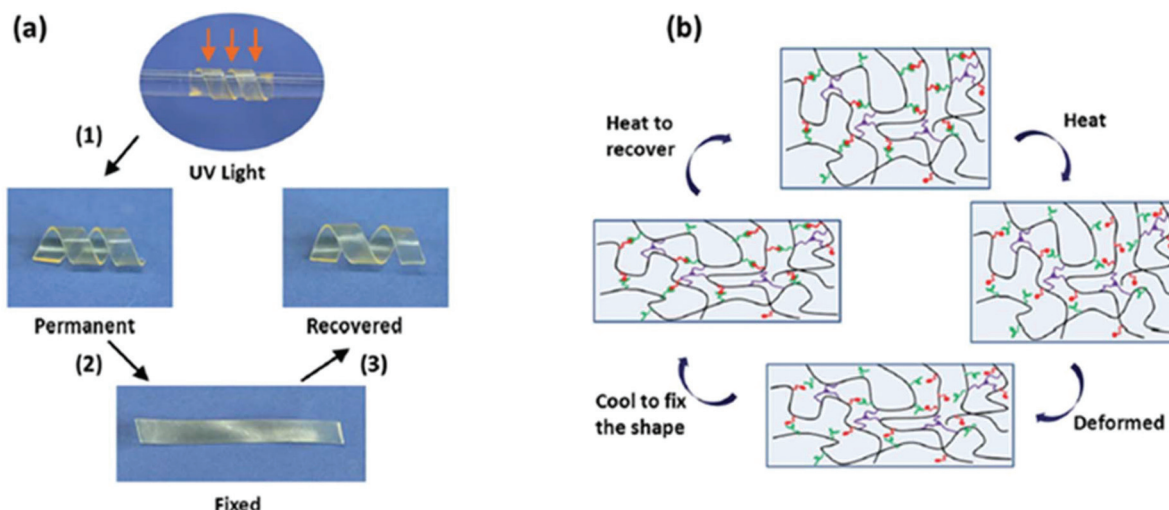


Fig. 15 (a) Photographs demonstrating the shape-memory behavior of an ionic rubber and (b) schematic evolution of non-covalent bonds during shape-memory cycles. Reproduced from ref. 115 with permission from the Royal Society of Chemistry, copyright 2015.

design multifunctional rubber materials with excellent shape-memory properties as characterized by both  $R_f$  and  $R_r$  above 95% (Fig. 15).<sup>115</sup> The shape-memory behavior was achieved using reversible ionic crosslinks between carboxylic acid and amine groups to fix the temporary shape and covalent crosslinks to recover its permanent shape. A shape memory mechanism was then proposed: the dynamic ionic bonds break upon heating so that the material can be deformed. When the deformed material is cooled down, the ionic bonds reform, thus locking the temporary shape. Reheating will break again the reversible association in the temporary shaped sample, so that the stored strain is released and the sample returns to the permanent shape driven by the recovery stress arising from the covalently cross-linked network. Taking advantage of both electrostatic and hydrogen interactions, and soft/hard segment dissociation, ionic PU also present interesting thermally activated shape-memory behavior. Indeed, distinction of soft and hard segments on PU chains improves shape memory, while ionic clusters within hard segments act as fixing agents.<sup>133,134</sup> Interestingly, Peng *et al.* confirmed the role of ionic cluster size and energy level in thermally triggered shape memory by designing polymethacrylate-based polyelectrolytes bearing carboxylic acid and amine groups (Fig. 16).<sup>108</sup> Note that the size of ionic clusters is proportionally related to their strength since increasing the amount of ionic interactions allows a better charge delocalization, and thus more stable interactions. Such a system enables multi-shape memory functions as the strongest ionic interactions (*i.e.* largest ionic clusters) act during the stationary phase to prevent chain relaxation and memorize the permanent shape, whereas the weakest ionic interactions (*i.e.* small ionic clusters and free ions) form temporary networks and store strain energy after shape fixing. Ionic hybrids with attractive thermally induced shape-memory properties have been further developed by Odent *et al.*<sup>14</sup> Therein, synthesizing ionic hybrids made of blends of cationic

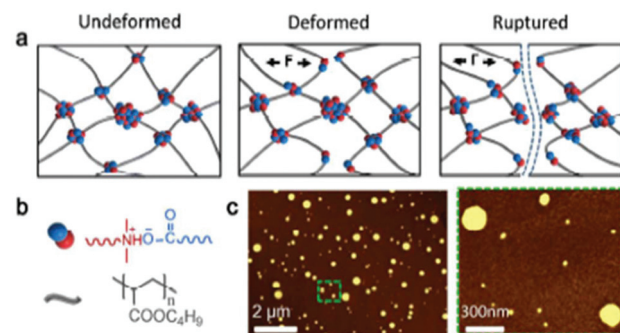


Fig. 16 (a) Schematic evolution of a non-covalent network under stretching, (b) electrostatic interactions and the chain backbone, and (c) AFM phase diagram of ionic polymethacrylate. Reproduced from ref. 108 with permission from the Royal Society of Chemistry, copyright 2018.

imidazolium-terminated oligomers and anionic sulfonate functionalized silica nanoparticles within commercial polylactide led to  $R_f$  and  $R_r$  up to 100 and 79%, respectively. In this work, electrostatic interactions between polymeric and particle partners endowed the creation of a transient network that governed the significant shape memory behavior observed. Importantly, the overall morphology and the specific location of silica nanoparticles were consistent with optimized ionic interactions between the sulfonate and imidazolium groups.

Water-induced (or moisture-induced) shape memory materials have recently gained interest based on the mild conditions to trigger shape recovery. Compared to thermally activated shape-memory materials, moisture sensitive shape-memory opens a new door for future biomedical applications such as body implants, or controlled drug release. This water-induced shape-memory behavior relies on the penetration of water molecules within amorphous areas, thus leading to a significant change of

mobility due to the plasticizing effect. Working on zwitterionic PU, Zhuo *et al.* managed to reconfigure the permanent shape during a shape-fixation sequence by applying water treatment on the thermally deformed shape.<sup>135</sup> By exposing the material to water, cationic and anionic moieties dissociate and both soft and hard PU segments are rearranged. The authors also showed that the recovery speed was proportionally related to relative humidity. Finally, the shape-memory behavior of these zwitterionic polyurethanes could be both thermally and water activated under human body conditions.<sup>136</sup> Li *et al.* also reported a water-triggered shape-memory behavior for a zwitterionic polymer.<sup>137</sup> Again, moisture absorption led to breaking of ionic interactions and a plasticizing effect, which allows an improved strain release and recovery to the permanent shape.

Like water-triggered shape memory properties, pH responsiveness can offer many biomedical applications.<sup>138</sup> pH-Responsive shape memory has recently been observed for polyampholytes made of sodium *p*-styrenesulfonate, methacrylic acid and 3-(methacryloylamino)propyltrimethylammonium chloride.<sup>139</sup> Shape memory mechanism is herein triggered by immersion in NaOH solution after fixation into HCl solution (Fig. 17). The shape memory can be repeated many times thanks to spontaneous twisting after new exposition to HCl. Swelling kinetics and residual stress are responsible for this last phenomenon, while bonding and rupture of carboxylate–ammonium interactions govern the shape memory mechanism.

Among all its appealing applications, shape-memory properties can be applied to improve or activate a self-healing mechanism. This so-called shape-memory assisted self-healing (SMASH) has been mentioned a few times in the literature.<sup>140,141</sup> During a SMASH process, the activation of the shape-memory effect can bring the cracked surfaces back together (zipping), thus making molecular diffusion possible for self-healing.<sup>142</sup> SMASH can be a pathway to heal large fracture (especially for coatings) by a zipping/rebonding two-step process. To the best of our knowledge, no ion-based materials have currently shown SMASH properties. However, we expect that the combination of self-healing and shape-memory properties exhibited by numerous ionic polymer materials could lead to the development of SMASH behavior.

## 5.2. Self-healing

Depending on the application, polymeric materials can be subjected to several constraints, environmental conditions, ageing

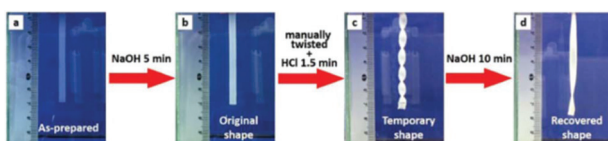


Fig. 17 Example of pH responsive shape-memory by Zhang *et al.* From left to right: (a) as-prepared; (b) original shape after treatment in 0.1 M NaOH; (c) fixed temporary shape in 0.1 M HCl; and (d) recovered shape in 0.1 M NaOH. Reprinted with permission from ref. 139. Copyright 2018, John Wiley & Sons, Inc.

factors, *etc.* that may compromise materials and structural integrity with various consequences from being harmful to users to causing economical loss. Self-healing materials which have the ability to repair themselves and recover functionality after damage are therefore highly appealing. Herein, dynamic ionic interactions surely represent an effective way to endow the resulting ionic polymeric materials with self-healing characteristics. In other terms, self-healing properties can be conferred by weak ionic interactions due to their relatively short bond-exchange time and fast reforming process. For instance, Das *et al.* developed imidazolium functionalized rubber with self-healing ability at room temperature.<sup>143</sup> While self-healing at room temperature is rare for non-dynamic materials, addition of ionic dynamic interactions allows overcoming this limitation. By increasing temperature, though, the elevated chain mobility increases, thus improving healing efficiency. Similar temperature-dependence on self-healing materials was observed on polyampholyte hydrogels by Ihsan *et al.* (Fig. 18).<sup>144</sup> Herein, a higher ionic bond fraction and lower covalent crosslinking is seen as a means to enhance self-healing efficiency. Other authors referred to room-temperature self-healable zwitterion-based hydrogels based on sulfonate–amine or carboxylate–amine interactions.<sup>145,146</sup> Besides, hydrogels with time-independent healing efficiency have been presented by Bai *et al.*<sup>146</sup> In such a system, the time lapse (up to 24 h) between cutting and putting back together the two parts of the material does not influence healing efficiency. The latter time-independent healing efficiency is attributed to the absence of the local reconfiguration of the surface due to stable hydration.

Although polymeric self-healing (nano)composites have great potential, the healing performance is still limited because the segmental motion is slowed down by the presence of (nano)particles. An alternative to confer self-healing to (nano)composites was found in the function of particle surface modification chemistry to achieve enhanced polymer–particle interactions. Following such a strategy, Zheng *et al.* grafted poly(2-dimethylaminoethyl methacrylate) on silica nanoparticles and dispersed them into poly(acrylic acid), achieving a healing efficiency of *ca.* 100% after 12 h at room temperature compared to 50% without functionalization of silica.<sup>147</sup> Likewise, Odent *et al.* designed sulfonate modified silica nanoparticles and dispersed them into imidazolium-functionalized poly(ethylene glycol)-based PU to endow the material with self-healing ability upon heating for *ca.* 5 h at 50 °C.<sup>95</sup> Ionic polymeric systems also allow water (or other solvent)-induced self-healing.<sup>144</sup> It is worth mentioning that moisture can act as a local plasticizer at the cut surfaces, increasing local mobility and liberating free ionic groups to heal local damage.<sup>137</sup> For instance, Wen *et al.* designed zwitterionic PU bearing pyridinium and sulfonate moieties.<sup>148</sup> Within such systems, a high zwitterion amount led to higher self-healing performance (from *ca.* 45 to 100% by doubling the sulfonate function amount) due to higher charge density on the damaged surface. The chain mobility of ionomers and polyelectrolytes is not only temperature-dependent but is also affected by the salt concentration and type. Spruijt *et al.* and Ali *et al.* found that

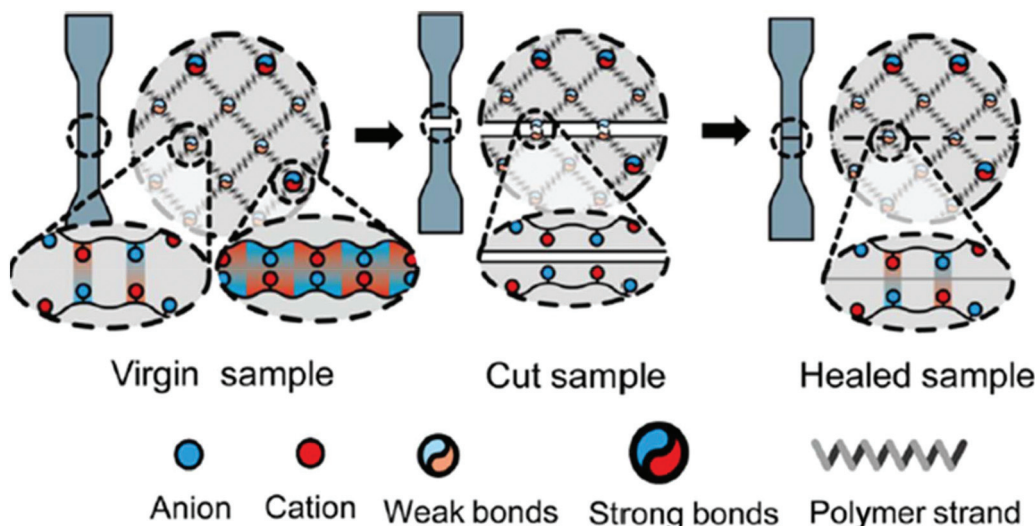


Fig. 18 Self-healing mechanism for ionic polymer systems. Reprinted with permission from ref. 144. Copyright 2016, American Chemical Society.

Published on 04/13/2019. Downloaded on 03/11/2020 02:31:30 ..

some polyelectrolyte complexes not only obey the time-temperature superposition (TTS) principle, but also time-salt superposition (TSS) (meaning that equivalent mechanical properties can be obtained by shifting frequencies for different salt concentrations), and time-ionic strength superposition (TISS). This opens a pathway to easily tune chain mobility based on the salt concentration and types.<sup>149–151</sup> For instance, Zacharia's group highlighted that the self-healing properties of a poly(ethylene imine)/poly(acrylic acid) complex could be modified by exposing the material to different salts.<sup>152,153</sup> While NaCl treatment screens charges resulting in an improvement of chain mobility and self-healing ability, the use of transition metal ion containing salts such as CuCl<sub>2</sub> forms new crosslinks (ionic interactions and coordination bonds) which worsen self-healing. Likewise, Li *et al.* presented self-healing zwitterionic-based polymethacrylate and reported the influence of salt on healing efficiency.<sup>137</sup> Adding NaCl salt increased the ionic exchange rate, which in turn led to higher strain at break after self-healing treatment due to destabilization of the polyion complex, also called an antipolyelectrolyte effect. This effect may not be an improvement of steady-state healing but rather a faster healing process due to an increased exchange probability with the polymer and salts. Finally, Yang *et al.* presented an ionically modified aerogel (*i.e.* extremely low density material made of open-nanoporous 3D networks) that is able to heal when cut surfaces are spread by water, thus promoting a surface rearrangement due to ionic interaction dissociation, increasing contact area and ionic exchange probability.<sup>154</sup> The final material not only healed but was also reinforced due to higher local ionic crosslink density after re-association of electrostatic interactions.

### 5.3. Energy dissipation

The constant rearrangement of ionic interactions gives opportunity to materials to dissipate energy under mechanical

testing or thermal treatment. Such a dissipative process allows potential applications in *e.g.* the automotive industry as components of bumpers, or as ballistic protections.<sup>78,80,82</sup> Under stretching, ionic polymeric chains usually align along the stretching direction, concentrating mechanical energy. The rupture of ionic bonds thereby allows polymeric chains to dissipate mechanical energy and relax before reattaching with other oppositely charged sites. The latter is well illustrated in the literature with the example of ionic hydrogels.<sup>8,155,156</sup> Besides, the broad range of accessible energy levels available in the case of ionic interactions offers many design opportunities for these ionic polymers as energy dissipation systems. That is, ionic bonds break and reform so that the materials are endowed with a high level of dissipated energy, as well as high toughness and fatigue resistance thanks to the fast and constant reversible exchanges. Among others, Xu *et al.* evidenced the key role of physical and/or chemical crosslinks in energy dissipation mechanisms within dual network hydrogels using latex particles as physical crosslinks.<sup>157</sup> During the loading-unloading process, the resulting dual network hydrogels dissipated a higher level of energy than a separated purely chemical and physical hydrogel combination. Physical interactions (*i.e.* ionic and hydrogen bonds) are herein envisioned to break at a low strain level, dissipating the major part of the energy, while chemical crosslinks (*i.e.* covalent bonds) tend to break due to finite elongation capacity. Comí *et al.* also quantified the tensile energy dissipation during the loading-unloading cycle of polyurethanes bearing tertiary amines and carboxylic acids.<sup>8</sup> Herein, short chain acids and equimolar amine/acid ratios enable a higher level of energy dissipation. Besides, the energy dissipation exponentially increases with the imposed strain on loading-unloading process. It is worth mentioning that the ability to dissipate energy is directly linked to the density of ionic moieties in the polymeric system. This phenomenon can be highlighted through the strain-rate

dependency of mechanical characteristics. Such a strain-dependence was further observed by Odent *et al.* using ionic nanocomposites that leverage the electrostatic interactions between imidazolium-functionalized PUs and sulfonate surface-modified silica nanoparticles<sup>95</sup> as well as by Deschanel *et al.* using either an ethylene methacrylic acid copolymer or ethylene methacrylic butyl acrylate copolymer.<sup>158</sup> As such, Young's modulus, yield strength and, very uncommonly, elongation at break increase simultaneously with the strain rate. Authors assumed that the strain-rate behavior is the result of the ionic nature of the system with the relaxation rate of these dynamic crosslinks probably in the range of applied strain rates. Potaufoux *et al.* further designed ultra-tough PLA-based ionic nanocomposites and presented a detailed mechanistic study aiming at elucidating the energy-dissipative toughening (up to 25-fold increase compared to neat PLA) under quasi-static and high speed loadings (Fig. 19).<sup>155</sup> The high toughness is especially due to the morphology, maximizing electrostatic interactions between the sulfonate and imidazolium groups on the silica and PU chains, respectively.

#### 5.4. Ionic conductivity

Ionic conductivity is a fundamental property that involves the motion of free ions within the material. As such, counterion migration in ionic polymeric materials endows the materials with high ionic conductivity depending on the nature and size of the involved counterions. First sighting of ionically conductive polymeric systems appeared on incorporating various salts

into swollen hydrogels.<sup>55,159</sup> Recall that water acted as a plasticizer, improving free-ion motion and chain mobility, to confer conductive behavior. Ionic composite hydrogels that leverage electrostatic interactions between sulfonate surface-modified silica nanoparticles and ammonium-containing hydrogels revealed an ionic conductivity of  $2.9 \text{ S m}^{-1}$  for a low voltage of 50 mV (ionic conductivity improved 1000 times compared to that of the reference polyacrylamide), which is related to the presence of their mobile counterions,  $\text{Na}^+$  and  $\text{Cl}^-$ , respectively.<sup>160</sup> Note that, it is commonly admitted that ionic conductivity above  $0.1 \text{ S m}^{-1}$  is necessary for the development of advanced applications such as batteries.<sup>161</sup> In addition, owing to the high ionic conductivity, the resulting ionic composite hydrogels can be rapidly 3D-printed at high resolution using commercial stereolithography technology, providing opportunities for a variety of practical applications such as actuators, compliant conductors and sensors for *e.g.* soft robotics (Fig. 20). Similarly, Liu *et al.* designed a 3D printed double-network hydrogel combining crosslinked  $\kappa$ -carrageenan ionically interacting with covalently crosslinked polyacrylamide of high conductivity and excellent electrical restoration after healing (>99%).<sup>162</sup> In order to improve conductivity and avoid any undesired swelling due to water absorption, aqueous solutions are progressively replaced with ionic liquids. For instance, Shen *et al.* synthesized a crosslinked poly(ionic liquid) with an imidazolium backbone and bis(trifluoromethane sulfonimide) counterions.<sup>163</sup> An electro-responsive actuator was further designed by implementing this as-synthesized poly(ionic liquid) between two carbon nanotube sheets. The resulting actuator bent on applying a voltage as a result of charge accumulation on one of the carbon nanotube sheets due to ion transport. They further showed that the ionic conductivity decreased with the crosslink density and the hydrophobicity of the poly(ionic liquid), resulting in a reduced performance of the actuator. Sensors have been further designed by using the high conductivity of ionic polymeric materials (Fig. 21). For instance, Liao *et al.* developed an imidazolium-based poly(ionic liquid) with acetate as free anions.<sup>164</sup> Herein, thermo-dependent conductivity (15% increase of conductivity by heating of only 1 °C) was observed in the same way as conductivity increasing with temperature for ionic liquids. Taking advantage of this property, authors

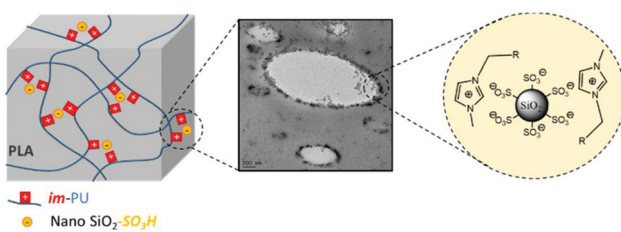


Fig. 19 Design of ultra-tough PLA-based ionic nanocomposites, based on polymer/particle ionic interactions with impact of a modifier-like morphology. Adapted from ref. 155. Copyright 2020 with permission from Elsevier.

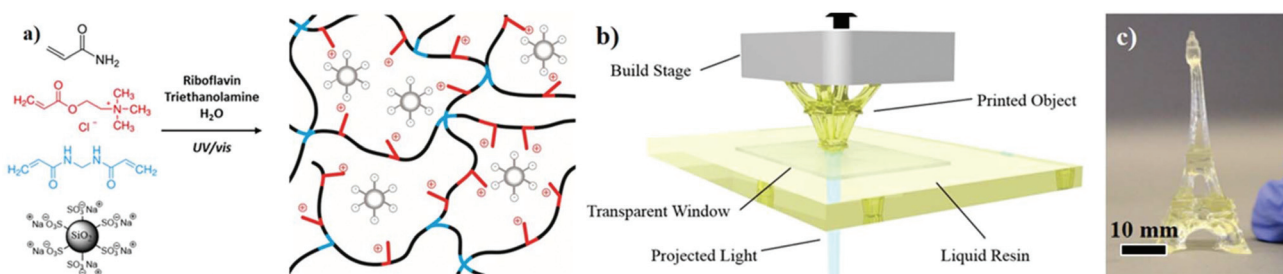
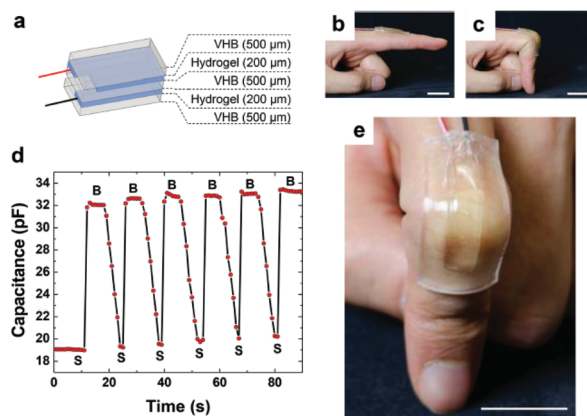


Fig. 20 (a) Chemistry of ionic composite hydrogels via photo-polymerization; (b) fast bottom-up fabrication of high-resolution features from the chemistry above using stereolithography; and (c) 3D printed Eiffel Tower. Adapted with permission from ref. 160. Copyright 2017, John Wiley & Sons, Inc.



**Fig. 21** Ionic polymer as part of a device for designing ionic skin. (a) A strain sensor is fabricated by sandwiching a layer of a stretchable dielectric between two layers of a stretchable ionic conductor (salt-containing hydrogel), which are then connected to two metallic electrodes. (b) The strain sensor is attached to a straight finger. (c) The bending of the finger stretched the strain sensor. (d) The capacitance is measured as the finger bent repeatedly. (e) The strain sensor was fully transparent. The scale bars in (b), (c) and (e) are 2 cm. Reprinted with permission from ref. 180. Copyright 2014, John Wiley & Sons, Inc.

designed an electronic sensor based on the thermal sensing performance which could be used to monitor body temperature. Similarly, Darabi *et al.* designed multicomponent hydrogels with tunable conductivity depending on the compression strength by combining ionic interactions and metal-ligand coordination.<sup>165</sup> Although the design is highly conductive in the presence of ferric ions, ionic components aimed to avoid ferric aggregates and improved free-ion motion. By introducing this metallic hydrogel between two poly(dimethylsiloxane) membranes, a wireless motion sensor was produced.

## 6. Applications of ionic polymeric materials

The broad range of properties and stimuli-responsiveness of ionic polymeric materials offers many applications in different fields, including soft robotics (*e.g.* such as sensors, actuators or membranes),<sup>16,166,167</sup> biomedical applications,<sup>168</sup> water treatment,<sup>169</sup> or energy storage.<sup>170</sup> Recently, the rise of soft robotics has led to the design of biomimetic actuators and artificial muscles.<sup>19,125,163</sup> In general, actuators are devices that can convert an external stimulus to mechanical motion. Taking advantage of the multiple shape-memory behaviors of ionomers, many actuators were designed using ionic polymeric materials. For instance, Shen *et al.* created a Nafion®-based actuator which is able to bend, twist or oscillate under electrical and thermal stimuli.<sup>171,172</sup> While Nafion® is often used as an electrolyte, the nature of electrodes can vary in order to improve interface efficiency and ion mobility. Thus, Ru *et al.* developed an electroactive actuator made of two nanoporous carbon nanotube sheets and a mixture of Nafion® and imidazolium-based ionic liquid as the electrolyte.<sup>173</sup> Other authors

referred to poly(3,4 ethylenedioxythiophene)-poly(styrenesulfonate) (PEDOT-PSS)<sup>174</sup> or nanodispersed platinum salt<sup>175</sup> to enhance the ionic conductivity at the interface between the electrodes and electrolyte. Khan *et al.* chose poly(1,4-phenylene ether-ether sulfone) (containing no fluorine unlike Nafion®) to design ionic polymer–metal composite actuators, showing large and fast deformation in response to electrical stimuli for artificial muscle applications.<sup>176,177</sup> With sulfonate-functionalized chitosan, Jeon *et al.* developed a biobased actuator by optimizing ionic interactions among chitosan, the ionic liquid and graphene oxide (Fig. 22).<sup>178</sup> Despite the rise of ionic polymeric materials as actuators, the latter is often found suffering from limitations such as fatigue resistance, water retention and strong adhesion with other components (like hydrophobic elastomers) which can deteriorate actuator efficiency with time.<sup>166</sup> In the field of soft-robotics, sensors also represent one of the main applications of ionic polymeric materials. Among sensors, so-called ionic skin referred to devices able to detect environmental stimuli (*e.g.* heat, pressure, and moisture) while protecting skin or other tissues.<sup>179</sup> For instance, Darabi *et al.* combined highly conductive polypyrrole with a tough DN-hydrogel in order to design a pressure-sensitive device for human motion detection.<sup>165</sup> Likewise, Liu *et al.* built a strain sensor based on a DN-hydrogel, showing excellent conductive stability and electrical restoration performance (>99%).<sup>162</sup> Covalently crosslinked polyacrylamide hydrogels are often associated with salts (NaCl and LiCl) to develop highly ionic conductive pressure-sensitive ionic touch panels.<sup>180,181</sup> Since ionic skin is often designed with ionic hydrogels (or hydrogels containing free-ions), these devices suffer from poor environmental stability. Therefore, one of the future challenges is to overcome unstable hydration, swelling, and possible ion leakage in an aqueous environment.<sup>182</sup> Poly(ionic liquid)s also represent interesting candidates for designing other sensing devices as they are highly conductive while becoming even more conductive upon an increase of temperature.<sup>164</sup> The ability of ionic polymeric

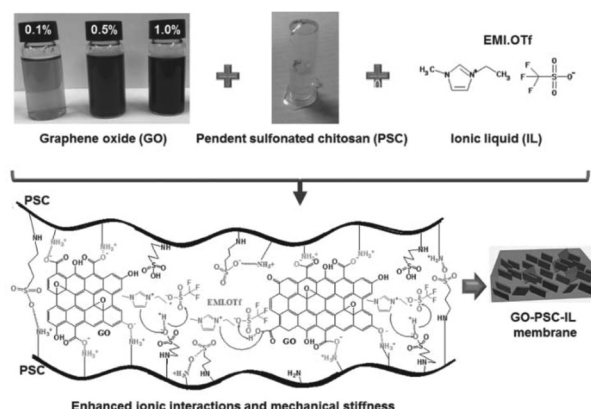


**Fig. 22** Biobased membrane with enhanced ionic interactions for the design of artificial muscles. Reprinted with permission from ref. 178. Copyright 2013, John Wiley & Sons, Inc.

materials to sense or transmit a signal not only refers to their ionic conductivity, but can also take advantage of pH, solvent or other responsiveness.<sup>183,184</sup> For instance, a carbon disulfide sensor (accuracy of a few ppm) was designed by Saha *et al.* using a leucine-based polyampholyte showing red luminescence in the presence of CS<sub>2</sub>.<sup>185</sup> Sun *et al.* developed an ultra-sensitive weak-acid detector (with an acetic acid concentration up to 10<sup>-6</sup> mol L<sup>-1</sup>) based on a porous structure made of an imidazolium-based PIL.<sup>186</sup> For specific biomarker detection, Chou *et al.* designed a PZw hydrogel that could be functionalized with antibodies for potential diagnostic applications.<sup>187</sup>

It is worth mentioning that ionic hydrogels are well-used in biomedical applications as they show biocompatibility, low cytotoxicity and antimicrobial properties. One of the most promising pathways for application of ionic polymeric materials in the biomedical fields regroups drug,<sup>119,188,189</sup> gene,<sup>190,191</sup> nucleic acid<sup>192</sup> and protein<sup>193</sup> delivery. Incorporating a zwitterionic sequence within polypeptides,<sup>194</sup> adding phosphonium groups into PEG-based hydrogels,<sup>195</sup> or functionalizing chitosan-PEG nanoparticles<sup>196</sup> are among recent strategies to design drug delivery systems. Besides, polyethyleneimines and phosphonium-based ionomers depict non-viral vectors to target tumors or cancers as they show high cellular uptake efficiency and easy assembly with small interfering RNA through electrostatic interactions.<sup>197-199</sup> For tissue engineering, tough hydrogels made of polyacrylamide, alginate, chitosan, and ionic polymethacrylates were recently investigated for such applications.<sup>1,200</sup> Indeed, combining chitosan and sodium alginate further allows the design of biocompatible and biodegradable ionic hydrogels used for biomedical applications such as cell growth,<sup>201</sup> cartilage reconstruction<sup>202</sup> or wound dressing.<sup>203</sup> Since one of the keys to design tissue engineering scaffolds is to minimize cytotoxicity and maximize cell adhesion so that tissues could adhere and be regenerated, polyampholyte hydrogels can also represent excellent candidates for tissue engineering.<sup>168,204</sup> Besides, a layer-by-layer method was often used to precisely design biomedical scaffolds from polyampholytes and ionic hydrogels for potential applications as cell culture devices, and also as nanocarriers and biosensors.<sup>205-207</sup> Future challenges for many ionic polymer materials in the biomedical fields will be deeper investigation of responsive properties in an *in vivo* environment.<sup>168,204</sup>

The development of ionic polymeric materials also led to numerous water-treatment applications by designing membranes, leveraging electrostatic interactions to remove heavy metals, nanoparticles or even amino acids.<sup>208-213</sup> Layer-by-layer assembly of oppositely charged polyelectrolytes probably represents a simple method to design membranes with efficient selectivity against heavy metal cations, large tunability and pH-responsiveness.<sup>214,215</sup> Many authors further reported the grafting of zwitterionic species as an efficient pathway to enhance water flux and antifouling performances, showing great filtration efficiency with regard to proteins.<sup>169,216</sup> Another method to create selective membranes relies on the assembly of particles that are fully or partially made of

polyelectrolytes.<sup>217,218</sup> pH and ionic strength responsiveness of polyelectrolytes enables precise control of particles and pore size of such membranes, and thus excellent size-selective filtration. To solve water pollution issues, biocatalytic membranes were further developed by immobilizing enzymes like trypsin or laccase on polyelectrolyte membranes to show high efficiency against micropollutants (e.g. bisphenol A), inorganic salts and proteins.<sup>219,220</sup> Note that, the well-known antifouling properties of some ionic polymeric materials give them a clear advantage to be designed as commercial membranes. However, the current challenge for the use of ionic polymeric materials as membranes is to achieve nanofiltration efficiency and selectivity.

Polyelectrolyte membranes are not only used for biomedical and environmental applications but can also be applied to electrochemical devices such as batteries, and fuel or solar cells.<sup>221,222</sup> Concerning fuel cell applications, proton exchange membranes require high proton conductivity, low methanol permeability and high chemical and thermal stability under operating conditions. Note that the simple exchange of counterions and ionic moieties for polyelectrolytes allows maximizing of fuel cell performances.<sup>223</sup> Nafion® was among the first ionic polymers used as proton exchange membranes, though, limited to operating temperatures below 80 °C due to some losses related to water evaporation.<sup>224</sup> Note that, the common use of water is still one of the major limitations to the use of ionic hydrogels as energy-storage devices. Besides, improvement of electrochemical and mechanical properties would also help develop new batteries and capacitors from ionic polymeric materials.<sup>225</sup> In order to improve proton conductivity, addition of nanofillers such as montmorillonite, or silica nanoparticles to ionic polymers has been proposed to enlarge applications for batteries and fuel cell applications.<sup>226,227</sup> Besides, poly(ionic liquid)s are also excellent candidates for such applications.<sup>228,229</sup> Poly(ionic liquid)s are recognized as good binders (*i.e.* materials ensuring good interface among the electrolyte, fuel and conductor) for fuel cells and lithium ion batteries.<sup>170</sup> Moreover, either highly conductive polyelectrolytes or poly(ionic liquid)s were utilized to immobilize electrolytes and improve lithium ion battery performances.<sup>225,230</sup> Finally, polyelectrolytes have recently found new application in the development of microbial fuel cells (*i.e.* fuel cells where fuel is replaced with microorganisms).<sup>231-233</sup> In addition to as-described applications, ionic polymeric materials can also be designed for textile,<sup>234,235</sup> packaging,<sup>236,237</sup> dentistry,<sup>238,239</sup> explosive,<sup>240</sup> CO<sub>2</sub> conversion,<sup>241-243</sup> and 3D printing<sup>244</sup> applications.

## 7. Conclusion and outlooks

Ionic interactions can undergo breaking and reformation in response to any immediate environmental change. Various ionic polymeric materials have been recently developed over the last few decades including: (1) ionomers, containing 1 to 15 mol% of ionic functions, (2) polyelectrolytes, containing

more than 10 to 15 mol% of ionic functions, and (3) ionic hydrogels, corresponding to physically crosslinked hydrogels bearing ionic motifs able to hold a large amount of water by swelling. The review first provides a deep understanding of the mechanistic pathways of electrostatic interactions within such ionic polymeric materials. The nature of ions and counterions, the related ionic strength and the addition of salts are among the key parameters controlling the overall performance of ionic systems. Herein, mechanistic models based of ionic hydrogels offer the possibility to fundamentally understand key parameters relative to reversible breaking and formation of ionic bonding. Besides, the structure–property relationships and characteristics of ionic polymeric materials are presented with respect to the underlying dynamic mechanisms, controlling the general performance of ionic polymeric materials. While the overall properties of ionomers appear to be mainly governed by the presence of ionic clusters due to their low ionic content, polyelectrolytes appeared to be more sensitive to the presence and the nature of salts (polyelectrolyte or anti-polyelectrolyte effects) when ionic hydrogels are highly dependent on the nature and density of their physical crosslinks. Finally, the present review further approached the stimuli-responsiveness of ionic polymeric materials, including shape-memory, self-healing, or energy dissipation. That is, ionic polymeric materials can be triggered by a wide range of stimuli including heat, water, pH and mechanical activation. All in all, ionic motifs provide opportunities for designing “smart” polymeric devices for various applications, including but not limited to, new actuators or sensors for soft robotics, biomedical implants or scaffolds for drug delivery or tissue engineering and membranes for environmental or energy applications. No doubt that in the foreseeable future, ionic polymeric materials will gain more and more importance in research fields, leading to development of new innovative applications.

## Conflicts of interest

There are no conflicts to declare.

## Acknowledgements

We gratefully acknowledge support from both the Wallonia and the European Commission “FSE and FEDER” in the frame of LCFM-BIOMASS project as well as the National Fund for Scientific Research (F.R.S.-F.N.R.S.) and the European Union’s Horizon 2020 research and innovation program under the BIODEST project (ID: 778092). We also acknowledge International Campus on Security and Transport Intermodality (CISIT), the Hauts de France Region, the European Community, the Regional Delegation for Research and Technology, the Ministry of Higher Education and Research and the National Center for Scientific Research for their financial support. J.-M. Ravez is a Research Associate for the F.R.S.-F.N.R.S.

## Notes and references

- Y. Liu, W. He, Z. Zhang and B. Lee, *Gels*, 2018, **4**, 46.
- N. Roy, B. Bruchmann and J.-M. Lehn, *Chem. Soc. Rev.*, 2015, **44**, 3786–3807.
- F. García and M. M. J. Smulders, *J. Polym. Sci., Part A: Polym. Chem.*, 2016, **54**, 3551–3577.
- B. Willocq, F. Khelifa, J. Brancart, G. Van Assche, Ph. Dubois and J.-M. Ravez, *RSC Adv.*, 2017, **7**, 48047–48053.
- I. Azcune and I. Odriozola, *Eur. Polym. J.*, 2016, **84**, 147–160.
- S. Delpierre, B. Willocq, G. Manini, V. Lemaur, J. Goole, P. Gerbaux, J. Cornil, P. Dubois and J.-M. Ravez, *Chem. Mater.*, 2019, **31**, 3736–3744.
- T. Li, Z. Xie, J. Xu, Y. Weng and B.-H. Guo, *Eur. Polym. J.*, 2018, **107**, 249–257.
- M. Comí, G. Lligadas, J. C. Ronda, M. Galià and V. Cádiz, *Eur. Polym. J.*, 2017, **91**, 408–419.
- Y. Furusho and T. Endo, *J. Polym. Sci., Part A: Polym. Chem.*, 2014, **52**, 1815–1824.
- J. Liu, D. Li, X. Zhao, J. Geng, J. Hua and X. Wang, *Polymers*, 2019, **11**, 492.
- S. Shinde, J. L. Sartucci, D. K. Jones and N. Gavvalapalli, *Macromolecules*, 2017, **50**, 7577–7583.
- S. C. Grindy, R. Learsch, D. Mozhdehi, J. Cheng, D. G. Barrett, Z. Guan, P. B. Messersmith and N. Holten-Andersen, *Nat. Mater.*, 2015, **14**, 1210–1216.
- J.-C. Lai, X.-Y. Jia, D.-P. Wang, Y.-B. Deng, P. Zheng, C.-H. Li, J.-L. Zuo and Z. Bao, *Nat. Commun.*, 2019, **10**, 1164.
- J. Odent, J.-M. Ravez, C. Samuel, S. Barrau, A. Enotiadis, P. Dubois and E. P. Giannelis, *Macromolecules*, 2017, **50**, 2896–2905.
- R. Dolog and R. A. Weiss, *Polymer*, 2017, **128**, 128–134.
- J. Kang, J. B.-H. Tok and Z. Bao, *Nat. Electron.*, 2019, **2**, 144–150.
- A. Ruiz de Luzuriaga, J. M. Matxain, F. Ruipérez, R. Martin, J. M. Asua, G. Cabañero and I. Odriozola, *J. Mater. Chem. C*, 2016, **4**, 6220–6223.
- B. Gyarmati, B. Á. Szilágyi and A. Szilágyi, *Eur. Polym. J.*, 2017, **93**, 642–669.
- L. Hu, Q. Zhang, X. Li and M. J. Serpe, *Mater. Horiz.*, 2019, **6**, 1774–1793.
- E. Van Ruymbeke, *J. Rheol.*, 2017, **61**, 1099–1102.
- M. Capelot, D. Montarnal, F. Tournilhac and L. Leibler, *J. Am. Chem. Soc.*, 2012, **134**, 7664–7667.
- W. Denissen, J. M. Winne and F. E. Du Prez, *Chem. Sci.*, 2016, **7**, 30–38.
- Y. Zhou, R. Groote, J. G. P. Goossens, R. P. Sijbesma and J. P. A. Heuts, *Polym. Chem.*, 2019, **10**, 136–144.
- J. L. Self, N. D. Dolinski, M. S. Zayas, J. Read de Alaniz and C. M. Bates, *ACS Macro Lett.*, 2018, **7**, 817–821.
- J. J. Lessard, L. F. Garcia, C. P. Easterling, M. B. Sims, K. C. Bentz, S. Arencibia, D. A. Savin and B. S. Sumerlin, *Macromolecules*, 2019, **52**, 2105–2111.

26 B. Hendriks, J. Waelkens, J. M. Winne and F. E. Du Prez, *ACS Macro Lett.*, 2017, **6**, 930–934.

27 J. P. Brutman, P. A. Delgado and M. A. Hillmyer, *ACS Macro Lett.*, 2014, **3**, 607–610.

28 R. L. Snyder, D. J. Fortman, G. X. De Hoe, M. A. Hillmyer and W. R. Dichtel, *Macromolecules*, 2018, **51**, 389–397.

29 W. Denissen, M. Drosesbeke, R. Nicolaïj, L. Leibler, J. M. Winne and F. E. Du Prez, *Nat. Commun.*, 2017, **8**, 14857.

30 L. Cao, J. Fan, J. Huang and Y. Chen, *J. Mater. Chem. A*, 2019, **7**, 4922–4933.

31 X. Niu, F. Wang, X. Kui, R. Zhang, X. Wang, X. Li, T. Chen, P. Sun and A. Shi, *Macromol. Rapid Commun.*, 2019, **40**, 1900313.

32 M. M. Obadia, A. Jourdain, P. Cassagnau, D. Montarnal and E. Drockenmuller, *Adv. Funct. Mater.*, 2017, **27**, 1703258.

33 S. Ciarella, F. Sciortino and W. G. Ellenbroek, *Phys. Rev. Lett.*, 2018, **121**, 58003.

34 H. Liu, H. Zhang, H. Wang, X. Huang, G. Huang and J. Wu, *Chem. Eng. J.*, 2019, **368**, 61–70.

35 I. Capek, *Adv. Colloid Interface Sci.*, 2005, **118**, 73–112.

36 L. D. Blackman, P. A. Gunatillake, P. Cass and K. E. S. Locock, *Chem. Soc. Rev.*, 2019, **48**, 757–770.

37 K. Mayumi, A. Marcellan, G. Ducouret, C. Creton and T. Narita, *ACS Macro Lett.*, 2013, **2**, 1065–1068.

38 R. Long, K. Mayumi, C. Creton, T. Narita and C.-Y. Hui, *Macromolecules*, 2014, **47**, 7243–7250.

39 X. Wang and W. Hong, *Soft Matter*, 2011, **7**, 8576.

40 C.-Y. Hui and R. Long, *Soft Matter*, 2012, **8**, 8209.

41 C. Y. Hui, J. Guo, M. Liu and A. Zehnder, *Int. J. Fract.*, 2019, **215**, 77–89.

42 A. D. Drozdov and J. de Claville Christiansen, *J. Mech. Behav. Biomed. Mater.*, 2018, **88**, 58–68.

43 M. Bacca, C. Creton and R. M. McMeeking, *J. Appl. Mech.*, 2017, **84**, 121009.

44 Y. Mao, S. Lin, X. Zhao and L. Anand, *J. Mech. Phys. Solids*, 2017, **100**, 103–130.

45 İ. D. Külcü, *Results Phys.*, 2019, **12**, 1826–1833.

46 K. Yu, A. Xin and Q. Wang, *J. Mech. Phys. Solids*, 2018, **121**, 409–431.

47 F. J. Vernerey, *J. Mech. Phys. Solids*, 2018, **115**, 230–247.

48 F. J. Vernerey, R. Long and R. Brighenti, *J. Mech. Phys. Solids*, 2017, **107**, 1–20.

49 J. M. Winne, L. Leibler and F. E. Du Prez, *Polym. Chem.*, 2019, **10**, 6091–6108.

50 Q. Chen, G. J. Tudry and R. H. Colby, *J. Rheol.*, 2013, **57**, 1441–1462.

51 P. Lin, S. Ma, X. Wang and F. Zhou, *Adv. Mater.*, 2015, **27**, 2054–2059.

52 Y. Miwa, J. Kurachi, Y. Kohbara and S. Kutsumizu, *Commun. Chem.*, 2018, **1**, 5.

53 H. Wu, J. M. Ting, O. Werba, S. Meng and M. V. Tirrell, *J. Chem. Phys.*, 2018, **149**, 163330.

54 E. Turkoz, A. Perazzo, C. B. Arnold and H. A. Stone, *Appl. Phys. Lett.*, 2018, **112**, 203701.

55 Z. Cao and G. Zhang, *Phys. Chem. Chem. Phys.*, 2015, **17**, 27045–27051.

56 H. M. Fares and J. B. Schlenoff, *J. Am. Chem. Soc.*, 2017, **139**, 14656–14667.

57 M. Yang, J. Shi and J. B. Schlenoff, *Macromolecules*, 2019, **52**, 1930–1941.

58 X. Lin and M. W. Grinstaff, *Isr. J. Chem.*, 2013, **53**, 498–510.

59 D. Bresser, S. Lyonnard, C. Iojoiu, L. Picard and S. Passerini, *Mol. Syst. Des. Eng.*, 2019, **4**, 779–792.

60 E. Spruijt, S. A. van den Berg, M. A. Cohen Stuart and J. van der Gucht, *ACS Nano*, 2012, **6**, 5297–5303.

61 Z. Zhang, Q. Chen and R. H. Colby, *Soft Matter*, 2018, **14**, 2961–2977.

62 T. K. Lytle, L.-W. Chang, N. Markiewicz, S. L. Perry and C. E. Sing, *ACS Cent. Sci.*, 2019, **5**, 709–718.

63 A. M. Rumyantsev, N. E. Jackson, B. Yu, J. M. Ting, W. Chen, M. V. Tirrell and J. J. de Pablo, *ACS Macro Lett.*, 2019, **8**, 1296–1302.

64 R. K. Bose, N. Hohlbein, S. J. Garcia, A. M. Schmidt and S. van der Zwaag, *Phys. Chem. Chem. Phys.*, 2015, **17**, 1697–1704.

65 J. R. Hemmer, B. P. Mason and R. Casalini, *J. Polym. Sci., Part B: Polym. Phys.*, 2019, **57**, 1074–1079.

66 L. M. Hall, M. J. Stevens and A. L. Frischknecht, *Phys. Rev. Lett.*, 2011, **106**, 127801.

67 B. Ma, T. D. Nguyen, V. A. Pryamitsyn and M. Olvera de la Cruz, *ACS Nano*, 2018, **12**, 2311–2318.

68 C. Huang, Q. Chen and R. A. Weiss, *Macromolecules*, 2017, **50**, 424–431.

69 L. M. Hall, M. E. Seitz, K. I. Winey, K. L. Opper, K. B. Wagener, M. J. Stevens and A. L. Frischknecht, *J. Am. Chem. Soc.*, 2012, **134**, 574–587.

70 Z. Zhang, C. Liu, X. Cao, J.-H. H. Wang, Q. Chen and R. H. Colby, *Macromolecules*, 2017, **50**, 963–971.

71 J. S. Enokida, V. A. Tanna, H. H. Winter and E. B. Coughlin, *Macromolecules*, 2018, **51**, 7377–7385.

72 J. S. Enokida, W. Hu, H. Fang, B. F. Morgan, F. L. Beyer, H. H. Winter and E. B. Coughlin, *Macromolecules*, 2020, **53**, 1767–1776.

73 Q. Zhao, C. Shen, K. P. Halloran and C. M. Evans, *ACS Macro Lett.*, 2019, **8**, 658–663.

74 Q. Chen, N. Bao, J.-H. H. Wang, T. Tunic, S. Liang and R. H. Colby, *Macromolecules*, 2015, **48**, 8240–8252.

75 A. Eisenberg and M. Rinaudo, *Polym. Bull.*, 1990, **24**, 671–671.

76 R. W. Rees and D. J. Vaughan, *Polym. Prepr. (Am. Chem. Soc., Div. Polym. Chem.)*, 1965, **6**, 287–295.

77 L. Lu and G. Li, *ACS Appl. Mater. Interfaces*, 2016, **8**, 14812–14823.

78 R. J. Varley and S. van der Zwaag, *Acta Mater.*, 2008, **56**, 5737–5750.

79 *Self healing materials: an alternative approach to 20 centuries of materials science*, ed. S. van der Zwaag, Springer, Dordrecht, 2007.

80 S. J. Kalista, J. R. Pflug and R. J. Varley, *Polym. Chem.*, 2013, **4**, 4910.

81 W. Post, R. Bose, S. García and S. van der Zwaag, *Polymers*, 2016, **8**, 436.

82 R. J. Varley, S. Shen and S. van der Zwaag, *Polymer*, 2010, **51**, 679–686.

83 M. W. Spencer, M. D. Wetzel, C. Troeltzsch and D. R. Paul, *Polymer*, 2012, **53**, 569–580.

84 X. Qiao and R. A. Weiss, *Macromolecules*, 2013, **46**, 2417–2424.

85 R. K. Bose, N. Hohlbein, S. J. Garcia, A. M. Schmidt and S. van der Zwaag, *Polymer*, 2015, **69**, 228–232.

86 X. Ma, J. A. Sauer and M. Hara, *Macromolecules*, 1995, **28**, 3953–3962.

87 B. P. Grady, *Polym. Eng. Sci.*, 2008, **48**, 1029–1051.

88 T. Xie, J. Li and Q. Zhao, *Macromolecules*, 2014, **47**, 1085–1089.

89 R. R. Kohlmeyer, M. Lor and J. Chen, *Nano Lett.*, 2012, **12**, 2757–2762.

90 L. R. Middleton, E. B. Trigg, L. Yan and K. I. Winey, *Polymer*, 2018, **144**, 184–191.

91 L. Ju, J. Pretelt, T. Chen, J. M. Dennis, K. V. Heifferon, D. G. Baird, T. E. Long and R. B. Moore, *Polymer*, 2018, **151**, 154–163.

92 W. R. Khan, N. Murdakes and C. J. Cornelius, *Polymer*, 2018, **142**, 99–108.

93 M. Colonna, C. Berti, E. Binassi, M. Fiorini, S. Sullalti, F. Acquasanta, M. Vannini, D. Di Gioia and I. Aloisio, *Polymer*, 2012, **53**, 1823–1830.

94 M. R. Kleczek, R. A. Whitney, A. J. Daugulis and J. S. Parent, *React. Funct. Polym.*, 2016, **106**, 69–75.

95 J. Odent, J.-M. Raquez, Ph. Dubois and E. P. Giannelis, *J. Mater. Chem. A*, 2017, **5**, 13357–13363.

96 J. van der Gucht, E. Spruijt, M. Lemmers and M. A. Cohen Stuart, *J. Colloid Interface Sci.*, 2011, **361**, 407–422.

97 *Polyelectrolyte complexes in the dispersed and solid state. 1: Principles and theory*, ed. M. Müller and A. G. Cherstvy, Springer, Berlin, 2014.

98 V. S. Rathee, A. J. Zervoudakis, H. Sidky, B. J. Sikora and J. K. Whitmer, *J. Chem. Phys.*, 2018, **148**, 114901.

99 V. S. Rathee, H. Sidky, B. J. Sikora and J. K. Whitmer, *J. Am. Chem. Soc.*, 2018, **140**, 15319–15328.

100 G. K. Wasupalli and D. Verma, *Int. J. Biol. Macromol.*, 2018, **114**, 10–17.

101 X. Sun, J. Shi, X. Xu and S. Cao, *Int. J. Biol. Macromol.*, 2013, **59**, 273–281.

102 Y. Song, K. P. Meyers, J. Gerringer, R. K. Ramakrishnan, M. Humood, S. Qin, A. A. Polycarpou, S. Nazarenko and J. C. Grunlan, *Macromol. Rapid Commun.*, 2017, **38**, 1700064.

103 A. J. Erwin, H. Lee, S. Ge, S. Zhao, V. F. Korolovich, H. He, K. Matyjaszewski, A. P. Sokolov and V. V. Tsukruk, *Eur. Polym. J.*, 2018, **109**, 326–335.

104 W. Zhang, Z. Kochovski, Y. Lu, B. V. K. J. Schmidt, M. Antonietti and J. Yuan, *ACS Nano*, 2016, **10**, 7731–7737.

105 Y. Wu, M. Regan, W. Zhang and J. Yuan, *Eur. Polym. J.*, 2018, **103**, 214–219.

106 F. Chen, J. Guo, D. Xu and F. Yan, *Polym. Chem.*, 2016, **7**, 1330–1336.

107 S. Kudaibergenov and N. Nuraje, *Polymers*, 2018, **10**, 1146.

108 Y. Peng, L. Zhao, C. Yang, Y. Yang, C. Song, Q. Wu, G. Huang and J. Wu, *J. Mater. Chem. A*, 2018, **6**, 19066–19074.

109 G. S. Georgiev, E. B. Kamenska, E. D. Vassileva, I. P. Kamenova, V. T. Georgieva, S. B. Iliev and I. A. Ivanov, *Biomacromolecules*, 2006, **7**, 1329–1334.

110 M. Ilčíková, J. Tkáč and P. Kasák, *Polymers*, 2015, **7**, 2344–2370.

111 M. Gao, K. Gawel and B. T. Stokke, *Eur. Polym. J.*, 2014, **53**, 65–74.

112 N. Sun, X. Gao, A. Wu, F. Lu and L. Zheng, *J. Mol. Liq.*, 2017, **248**, 759–766.

113 T. Yuan, X. Cui, X. Liu, X. Qu and J. Sun, *Macromolecules*, 2019, **52**, 3141–3149.

114 Y. Xu and D. Chen, *Mater. Chem. Phys.*, 2017, **195**, 40–48.

115 D. Wang, J. Guo, H. Zhang, B. Cheng, H. Shen, N. Zhao and J. Xu, *J. Mater. Chem. A*, 2015, **3**, 12864–12872.

116 M. Liu, J. Zhong, Z. Li, J. Rong, K. Yang, J. Zhou, L. Shen, F. Gao, X. Huang and H. He, *Eur. Polym. J.*, 2020, **124**, 109475.

117 Y. Zuo, Z. Jiao, L. Ma, P. Song, R. Wang and Y. Xiong, *Polymer*, 2016, **98**, 287–293.

118 E. Su, M. Yurtsever and O. Okay, *Macromolecules*, 2019, **52**, 3257–3267.

119 S. Afzal, M. Maswal and A. A. Dar, *Colloids Surf., B*, 2018, **169**, 99–106.

120 T. L. Sun, T. Kurokawa, S. Kuroda, A. B. Ihsan, T. Akasaki, K. Sato, Md. A. Haque, T. Nakajima and J. P. Gong, *Nat. Mater.*, 2013, **12**, 932–937.

121 K. Cui, T. L. Sun, T. Kurokawa, T. Nakajima, T. Nonoyama, L. Chen and J. P. Gong, *Soft Matter*, 2016, **12**, 8833–8840.

122 Y. Fan, W. Zhou, A. Yasin, H. Li and H. Yang, *Soft Matter*, 2015, **11**, 4218–4225.

123 R. Wang, Q. Yu, Y. He, J. Bai, T. Jiao, L. Zhang, Z. Bai, J. Zhou and Q. Peng, *J. Mol. Liq.*, 2019, **294**, 111576.

124 N. Yuan, L. Xu, B. Xu, J. Zhao and J. Rong, *Carbohydr. Polym.*, 2018, **193**, 259–267.

125 S. L. Banerjee, T. Swift, R. Hoskins, S. Rimmer and N. K. Singha, *J. Mater. Chem. B*, 2019, **7**, 1475–1493.

126 W. Zhao, L. Liu, F. Zhang, J. Leng and Y. Liu, *Mater. Sci. Eng., C*, 2019, **97**, 864–883.

127 T. Liu, T. Zhou, Y. Yao, F. Zhang, L. Liu, Y. Liu and J. Leng, *Composites, Part A*, 2017, **100**, 20–30.

128 M. Zare, M. P. Prabhakaran, N. Parvin and S. Ramakrishna, *Chem. Eng. J.*, 2019, **374**, 706–720.

129 S. Chen, F. Mo, F. J. Stadler, S. Chen, Z. Ge and H. Zhuo, *J. Mater. Chem. B*, 2015, **3**, 6645–6655.

130 H. Du, X. Liu, Y. Yu, Y. Xu, Y. Wang and Z. Liang, *Macromol. Chem. Phys.*, 2016, **217**, 2626–2634.

131 T. Calvo-Correas, A. Shirole, F. Crippa, A. Fink, C. Weder, M. A. Corcuera and A. Eceiza, *Mater. Sci. Eng., C*, 2019, **97**, 658–668.

132 K. A. Cavicchi, M. Pantoja and M. Cakmak, *J. Polym. Sci., Part B: Polym. Phys.*, 2016, **54**, 1389–1396.

133 P. K. Behera, P. Mondal and N. K. Singha, *Polym. Chem.*, 2018, **9**, 4205–4217.

134 S. Fu, H. Ren, Z. Ge, H. Zhuo and S. Chen, *Polymers*, 2017, **9**, 465.

135 H. Zhuo, H. Wen, G. Liu, H. Chen and S. Chen, *Polymer*, 2018, **158**, 25–31.

136 H. Zhuo, Z. Mei, H. Chen and S. Chen, *Polymer*, 2018, **148**, 119–126.

137 G. Li, Y. Wang, S. Wang, Z. Liu, Z. Liu and J. Jiang, *Macromol. Mater. Eng.*, 2019, **304**, 1800603.

138 Q. Song, H. Chen, S. Zhou, K. Zhao, B. Wang and P. Hu, *Polym. Chem.*, 2016, **7**, 1739–1746.

139 Y. Zhang, J. Liao, T. Wang, W. Sun and Z. Tong, *Adv. Funct. Mater.*, 2018, **28**, 1707245.

140 C. C. Hornat and M. W. Urban, *Prog. Polym. Sci.*, 2020, 101208.

141 E. D. Rodriguez, X. Luo and P. T. Mather, *ACS Appl. Mater. Interfaces*, 2011, **3**, 152–161.

142 W. Wu, J. Ekeocha, C. Ellingford, S. N. Kurup and C. Wan, in *Self-Healing Polymer-based Systems*, Elsevier, 2020, pp. 95–121.

143 A. Das, A. Sallat, F. Böhme, M. Suckow, D. Basu, S. Wiesner, K. W. Stöckelhuber, B. Voit and G. Heinrich, *ACS Appl. Mater. Interfaces*, 2015, **7**, 20623–20630.

144 A. B. Ihsan, T. L. Sun, T. Kurokawa, S. N. Karobi, T. Nakajima, T. Nonoyama, C. K. Roy, F. Luo and J. P. Gong, *Macromolecules*, 2016, **49**, 4245–4252.

145 H. Liu, C. Xiong, Z. Tao, Y. Fan, X. Tang and H. Yang, *RSC Adv.*, 2015, **5**, 33083–33088.

146 T. Bai, S. Liu, F. Sun, A. Sinclair, L. Zhang, Q. Shao and S. Jiang, *Biomaterials*, 2014, **35**, 3926–3933.

147 J. Zheng, P. Xiao, W. Liu, J. Zhang, Y. Huang and T. Chen, *Macromol. Rapid Commun.*, 2016, **37**, 265–270.

148 H. Wen, S. Chen, Z. Ge, H. Zhuo, J. Ling and Q. Liu, *RSC Adv.*, 2017, **7**, 31525–31534.

149 E. Spruijt, J. Sprakel, M. Lemmers, M. A. C. Stuart and J. van der Gucht, *Phys. Rev. Lett.*, 2010, **105**, 208301.

150 S. Ali and V. Prabhu, *Gels*, 2018, **4**, 11.

151 V. M. S. Syed and S. Srivastava, *ACS Macro Lett.*, 2020, **9**, 1067–1073.

152 H. Zhang, C. Wang, G. Zhu and N. S. Zacharia, *ACS Appl. Mater. Interfaces*, 2016, **8**, 26258–26265.

153 C. Li, Y. Gu and N. S. Zacharia, *ACS Appl. Mater. Interfaces*, 2018, **10**, 7401–7412.

154 J. Yang, L. Yi, X. Fang, Y. Song, L. Zhao, J. Wu and H. Wu, *Chem. Eng. J.*, 2019, **371**, 213–221.

155 J.-E. Potaufoux, J. Odent, D. Notta-Cuvier, R. Delille, S. Barrau, E. P. Giannelis, F. Lauro and J.-M. Raquez, *Compos. Sci. Technol.*, 2020, **191**, 108075.

156 J.-Y. Sun, X. Zhao, W. R. K. Illeperuma, O. Chaudhuri, K. H. Oh, D. J. Mooney, J. J. Vlassak and Z. Suo, *Nature*, 2012, **489**, 133–136.

157 J. Xu, X. Liu, X. Ren and G. Gao, *Eur. Polym. J.*, 2018, **100**, 86–95.

158 S. Deschanel, B. P. Greviskes, K. Bertoldi, S. S. Sarva, W. Chen, S. L. Samuels, R. E. Cohen and M. C. Boyce, *Polymer*, 2009, **50**, 227–235.

159 F. Bordi, C. Cametti and T. Gili, *Phys. Rev. E: Stat., Nonlinear, Soft Matter Phys.*, 2003, **68**, 11805.

160 J. Odent, T. J. Wallin, W. Pan, K. Kruemplerstaedter, R. F. Shepherd and E. P. Giannelis, *Adv. Funct. Mater.*, 2017, **27**, 1701807.

161 J. Shin, *Electrochem. Commun.*, 2003, **5**, 1016–1020.

162 S. Liu and L. Li, *ACS Appl. Mater. Interfaces*, 2017, **9**, 26429–26437.

163 C. Shen, Q. Zhao and C. M. Evans, *Adv. Mater. Technol.*, 2019, **4**, 1800535.

164 H. Liao, S. Liao, X. Tao, C. Liu and Y. Wang, *J. Mater. Chem. C*, 2018, **6**, 12992–12999.

165 M. A. Darabi, A. Khosrozadeh, R. Mbeleck, Y. Liu, Q. Chang, J. Jiang, J. Cai, Q. Wang, G. Luo and M. Xing, *Adv. Mater.*, 2017, **29**, 1700533.

166 C. Yang and Z. Suo, *Nature Reviews Materials*, 2018, **3**, 125–142.

167 H.-R. Lee, C.-C. Kim and J.-Y. Sun, *Adv. Mater.*, 2018, **30**, 1704403.

168 S. Haag and M. Bernards, *Gels*, 2017, **3**, 41.

169 H. Sun, Y. Zhang, H. Sadam, J. Ma, Y. Bai, X. Shen, J.-K. Kim and L. Shao, *J. Membr. Sci.*, 2019, **582**, 1–8.

170 F. N. Ajjan, M. Ambrogi, G. A. Tiruye, D. Cordella, A. M. Fernandes, K. Grygiel, M. Isik, N. Patil, L. Porcarelli, G. Rocasalbas, G. Vendramiutto, E. Zeglio, M. Antonietti, C. Detrembleur, O. Inganäs, C. Jérôme, R. Marcilla, D. Mecerreyes, M. Moreno, D. Taton, N. Solin and J. Yuan, *Polym. Int.*, 2017, **66**, 1119–1128.

171 Q. Shen, S. Trabia, T. Stalbaum, V. Palmre, K. Kim and I.-K. Oh, *Sci. Rep.*, 2016, **6**, 24462.

172 Q. Shen, T. Stalbaum, N. Minaian, I.-K. Oh and K. J. Kim, *Smart Mater. Struct.*, 2019, **28**, 015009.

173 J. Ru, C. Bian, Z. Zhu, Y. Wang, J. Zhang, T. Horiuchi, T. Sugino, X. Liu, H. Chen and K. Asaka, *Smart Mater. Struct.*, 2019, **28**, 085032.

174 S. Umrao, R. Tabassian, J. Kim, V. H. Nguyen, Q. Zhou, S. Nam and I.-K. Oh, *Sci. Robot.*, 2019, **4**, eaaw7797.

175 H. S. Wang, J. Cho, D. S. Song, J. H. Jang, J. Y. Jho and J. H. Park, *ACS Appl. Mater. Interfaces*, 2017, **9**, 21998–22005.

176 A. Khan, R. K. Jain and K. A. Alamry, *Polym.-Plast. Technol. Mater.*, 2020, **59**, 687–701.

177 A. Khan, R. K. Jain, P. Banerjee, B. Ghosh, Inamuddin and A. M. Asiri, *Sci Rep.*, 2018, **8**, 9909.

178 J.-H. Jeon, R. K. Cheedarala, C.-D. Kee and I.-K. Oh, *Adv. Funct. Mater.*, 2013, **23**, 6007–6018.

179 D. Jiang, Y. Wang, B. Li, C. Sun, Z. Wu, H. Yan, L. Xing, S. Qi, Y. Li, H. Liu, W. Xie, X. Wang, T. Ding and Z. Guo, *Macromol. Mater. Eng.*, 2019, **304**, 1900074.

180 J.-Y. Sun, C. Keplinger, G. M. Whitesides and Z. Suo, *Adv. Mater.*, 2014, **26**, 7608–7614.

181 C.-C. Kim, H.-H. Lee, K. H. Oh and J.-Y. Sun, *Science*, 2016, **353**, 682–687.

182 W. Xie, J. Duan, H. Wang, J. Li, R. Liu, B. Yu, S. Liu and J. Zhou, *J. Mater. Chem. A*, 2018, **6**, 24114–24119.

183 W. Zhang, Y. Li, Y. Liang, N. Gao, C. Liu, S. Wang, X. Yin and G. Li, *Chem. Sci.*, 2019, **10**, 6617–6623.

184 H. Lin, J. Gong, H. Miao, R. Guterman, H. Song, Q. Zhao, J. W. C. Dunlop and J. Yuan, *ACS Appl. Mater. Interfaces*, 2017, **9**, 15148–15155.

185 B. Saha, N. Choudhury, A. Bhadran, K. Bauri and P. De, *Polym. Chem.*, 2019, **10**, 3306–3317.

186 J.-K. Sun, W. Zhang, R. Guterman, H.-J. Lin and J. Yuan, *Nat. Commun.*, 2018, **9**, 1717.

187 Y.-N. Chou, F. Sun, H.-C. Hung, P. Jain, A. Sinclair, P. Zhang, T. Bai, Y. Chang, T.-C. Wen, Q. Yu and S. Jiang, *Acta Biomater.*, 2016, **40**, 31–37.

188 P. Xie and P. Liu, *Int. J. Biol. Macromol.*, 2019, **141**, 161–170.

189 D. Wu, L. Zhu, Y. Li, X. Zhang, S. Xu, G. Yang and T. Delair, *Carbohydr. Polym.*, 2020, **238**, 116126.

190 C. Jiang, J. Chen, Z. Li, Z. Wang, W. Zhang and J. Liu, *Expert Opin. Drug Delivery*, 2019, **16**, 363–376.

191 T. Park, J. Jeong and S. Kim, *Adv. Drug Delivery Rev.*, 2006, **58**, 467–486.

192 S. T. Hemp, A. E. Smith, J. M. Bryson, M. H. Allen and T. E. Long, *Biomacromolecules*, 2012, **13**, 2439–2445.

193 S. Ahmed, F. Hayashi, T. Nagashima and K. Matsumura, *Biomaterials*, 2014, **35**, 6508–6518.

194 S. Banskota, P. Yousefpour, N. Kirmani, X. Li and A. Chilkoti, *Biomaterials*, 2019, **192**, 475–485.

195 T. D. Harrison, P. J. Ragogna and E. R. Gillies, *Chem. Commun.*, 2018, **54**, 11164–11167.

196 M. Nag, V. Gajbhiye, P. Kesharwani and N. K. Jain, *Colloids Surf., B*, 2016, **148**, 363–370.

197 Y. Dai and X. Zhang, *Macromol. Biosci.*, 2019, **19**, 1800445.

198 A. Zakeri, M. A. J. Kouhbanani, N. Beheshtkhoo, V. Beigi, S. M. Mousavi, S. A. R. Hashemi, A. Karimi Zade, A. M. Amani, A. Savardashtaki, E. Mirzaei, S. Jahandideh and A. Movahedpour, *Nano Rev. Exp.*, 2018, **9**, 1488497.

199 S. T. Hemp, M. H. Allen, M. D. Green and T. E. Long, *Biomacromolecules*, 2012, **13**, 231–238.

200 K. M. Zurick and M. Bernards, *J. Appl. Polym. Sci.*, 2014, **131**, 40069.

201 K. Baysal, A. Z. Aroguz, Z. Adiguzel and B. M. Baysal, *Int. J. Biol. Macromol.*, 2013, **59**, 342–348.

202 E. Marsich, M. Borgogna, I. Donati, P. Mozetic, B. L. Strand, S. G. Salvador, F. Vittur and S. Paoletti, *J. Biomed. Mater. Res., Part A*, 2008, **84A**, 364–376.

203 R. Song, J. Zheng, Y. Liu, Y. Tan, Z. Yang, X. Song, S. Yang, R. Fan, Y. Zhang and Y. Wang, *Int. J. Biol. Macromol.*, 2019, **134**, 91–99.

204 M. T. Bernards, in *Switchable and Responsive Surfaces and Materials for Biomedical Applications*, Elsevier, 2015, pp. 45–64.

205 H. Yoon, E. J. Dell, J. L. Freyer, L. M. Campos and W.-D. Jang, *Polymer*, 2014, **55**, 453–464.

206 Y. Tan, U. H. Yildiz, W. Wei, J. H. Waite and A. Miserez, *Biomacromolecules*, 2013, **14**, 1715–1726.

207 A. Jafari, H. Sun, B. Sun, M. A. Mohamed, H. Cui and C. Cheng, *Chem. Commun.*, 2019, **55**, 1267–1270.

208 M. Boas, M. Burman, A. L. Yarin and E. Zussman, *Polymer*, 2018, **158**, 262–269.

209 Y.-L. Ji, W.-J. Qian, Q.-F. An, K.-R. Lee and C.-J. Gao, *J. Ind. Eng. Chem.*, 2018, **66**, 209–220.

210 T.-Z. Jia, J.-P. Lu, X.-Y. Cheng, Q.-C. Xia, X.-L. Cao, Y. Wang, W. Xing and S.-P. Sun, *J. Membr. Sci.*, 2019, **580**, 214–223.

211 K. D. Kelly, H. M. Fares, S. Abou Shaheen and J. B. Schlenoff, *Langmuir*, 2018, **34**, 3874–3883.

212 Y.-L. Ji, B.-X. Gu, Q.-F. An and C.-J. Gao, *Polymers*, 2017, **9**, 715.

213 W. Zhang, Q. Zhao and J. Yuan, *Angew. Chem., Int. Ed.*, 2018, **57**, 6754–6773.

214 R. M. DuChanois, R. Epsztein, J. A. Trivedi and M. Elimelech, *J. Membr. Sci.*, 2019, **581**, 413–420.

215 X. Li, C. Liu, W. Yin, T. H. Chong and R. Wang, *J. Membr. Sci.*, 2019, **584**, 309–323.

216 Y.-S. Guo, X.-D. Weng, B. Wu, Y.-F. Mi, B.-K. Zhu, Y.-L. Ji, Q.-F. An and C.-J. Gao, *J. Membr. Sci.*, 2019, **583**, 152–162.

217 R. Zhang, T. Zhou, H. Peng, M. Li, X. Zhu and Y. Yao, *J. Membr. Sci.*, 2019, **580**, 117–124.

218 K. Zhu, Y. Mu, M. Zhang, Y. Liu, R. Na, W. Xu and G. Wang, *J. Mater. Chem. A*, 2018, **6**, 7859–7870.

219 N. Dizge, R. Epsztein, W. Cheng, C. J. Porter and M. Elimelech, *J. Membr. Sci.*, 2018, **549**, 357–365.

220 S. Li, J. Luo and Y. Wan, *J. Membr. Sci.*, 2018, **549**, 120–128.

221 W. Qian, J. Texter and F. Yan, *Chem. Soc. Rev.*, 2017, **46**, 1124–1159.

222 Q. Zhao, Q. F. An, Y. Ji, J. Qian and C. Gao, *J. Membr. Sci.*, 2011, **379**, 19–45.

223 D. Mecerreyes, *Prog. Polym. Sci.*, 2011, **36**, 1629–1648.

224 A. Kusoglu and A. Z. Weber, *Chem. Rev.*, 2017, **117**, 987–1104.

225 Y. Guo, J. Bae, F. Zhao and G. Yu, *Trends Chem.*, 2019, **1**, 335–348.

226 I. Shabani, M. M. Hasani-Sadrabadi, V. Haddadi-Asl and M. Soleimani, *J. Membr. Sci.*, 2011, **368**, 233–240.

227 M. M. Hasani-Sadrabadi, E. Dashtimoghadam, F. S. Majedi and K. Kabiri, *J. Power Sources*, 2009, **190**, 318–321.

228 V. Atanasov, A. Oleynikov, J. Xia, S. Lyonnard and J. Kerres, *J. Power Sources*, 2017, **343**, 364–372.

229 O. Gil-Castell, R. Teruel-Juanes, F. Arenga, A. M. Salaberria, M. G. Baschetti, J. Labidi, J. D. Badia and A. Ribes-Greus, *React. Funct. Polym.*, 2019, **142**, 213–222.

230 F. Mo, H. Li, Z. Pei, G. Liang, L. Ma, Q. Yang, D. Wang, Y. Huang and C. Zhi, *Sci. Bull.*, 2018, **63**, 1077–1086.

231 J. Ma, N. Shi, Y. Zhang, J. Zhang, T. Hu, H. Xiao, T. Tang and J. Jia, *J. Power Sources*, 2020, **450**, 227628.

232 Y. Yang, M. Qin, X. Yang and Z. He, *J. Cleaner Prod.*, 2017, **168**, 1143–1149.

233 A. Reshetilov, Y. Plekhanova, S. Tarasov, S. Tikhonenko, A. Dubrovsky, A. Kim, V. Kashin, A. Machulin, G.-J. Wang, V. Kolesov and I. Kuznetsova, *Membranes*, 2019, **9**, 53.

234 Y. Y. F. Chan Vili, *Text. Res. J.*, 2007, **77**, 290–300.

235 S. Cao, M. N. Barcellona, F. Pfeiffer and M. T. Bernards, *J. Appl. Polym. Sci.*, 2016, **133**, 43985.

236 F. Şen, İ. Uzunsoy, E. Baştürk and M. V. Kahraman, *Carbohydr. Polym.*, 2017, **170**, 264–270.

237 P. Johnston and R. Adhikari, *Eur. Polym. J.*, 2017, **95**, 138–160.

238 S. Shahid and T. Duminis, in *Advanced Dental Biomaterials*, Elsevier, 2019, pp. 175–195.

239 F. Madi, S. K. Sidhu and J. W. Nicholson, *Dent. Mater.*, 2020, **36**, e9–e14.

240 B. Wang, Y. Feng, X. Qi, M. Deng, J. Tian and Q. Zhang, *Chem. – Eur. J.*, 2018, **24**, 15897–15902.

241 E. M. Maya, E. Verde-Sesto, D. Mantione, M. Iglesias and D. Mecerreyes, *Eur. Polym. J.*, 2019, **110**, 107–113.

242 Y. Chen, R. Luo, J. Bao, Q. Xu, J. Jiang, X. Zhou and H. Ji, *J. Mater. Chem. A*, 2018, **6**, 9172–9182.

243 Y. Xie, Q. Sun, Y. Fu, L. Song, J. Liang, X. Xu, H. Wang, J. Li, S. Tu, X. Lu and J. Li, *J. Mater. Chem. A*, 2017, **5**, 25594–25600.

244 H. Nulwala, A. Mirjafari and X. Zhou, *Eur. Polym. J.*, 2018, **108**, 390–398.